Master Thesis

Investigating the role of respiration in CO_2 outgassing from inland waters

University of Bremen

Faculty of Environmental Physics

Postgraduate Environmental Physics Program

Christodoulou Aliki

Matriculation number: 2991913

Date of birth: 10.03.1990

Examiners	Supervisors
Prof. Dr. Justus Notholt	Dr. Denise Müller-Dum
Prof. Mihalis Vrekoussis	Dr. Thorsten Warneke

Bremen, November 17, 2017

Abstract

Inland waters form an important link between terrestrial ecosystems, oceans and the atmosphere. They play a significant role in the global carbon cycle, because organic carbon in inland waters is transported, sequestered and decomposed to other inorganic forms (CO_2). The main mechanism that controls the CO_2 concentration in aquatic ecosystems is respiration. In this study the carbon dynamics of the largest river in Malaysia (Rajang River) is investigated. High dissolved organic carbon (DOC) concentrations were measured during two different campaigns, of which one took place in the wet and one in the dry season. The measured DOC was hypothesized to originate from disturbed soils and lateral inputs. A striking observation in the river DOC concentrations, which indicates the influence of anthropogenic disturbances in the river, is the high DOC values in the non-peat areas. Nevertheless, CO_2 concentrations were moderate compared to other peat-draining rivers. The second part of the study involves the development of a laboratory experiment to be able to determine the respiration rates and to be able to calculate rate coefficients. Due to an unexpected increase in DOC concentrations, a method was developed to account for this increase, to be still able to calculate the respiration rates. Furthermore, a comparison between the calculated respiration rates from the laboratory experiment and the calculated rates from the continuous in-situ measurements in the Weser River has been made. Although the experimental setup had several limitations, the calculated respiration rate coefficients are similar to those calculated based on the in-situ measurements.

Acknowledgements

First of all, I would like to thank my two supervisors Dr. Thorsten Warneke and Dr. Denise Müller-Dum for the guidance and continuous support they provided throughout my master thesis. The door of Dr. Thorsten Warneke office was always open whenever I ran into a trouble spot or had a question about my writing.

My gratitude also goes to my first and second examiners Prof. Dr. Justus Notholt and Prof. Mihalis Vrekoussis and to the whole working group for creating such a great working atmosphere. Especially, a very large thanks goes to Matthias Buschmann for his help in various Python problems and Hella van Asperen for her proof-reading and scientific improvements of my thesis. Both created such a nice working atmosphere and I was very glad to share an office with them.

Also I want to thank my Malaysian contact persons, most notably Prof. Dr. Moritz Müller for his organisation of the measurement campaign and for the support in the field measurements. Furthermore, I would like to thank all the people at ZMT who allowed me to use their working place for my experiment and supported me with the development of the experimental setup. I am very grateful to Dr. Antje Baum and Dr. Tim Rixen for their advice and help regarding the sampling and analyses.

Finally, I would like to thank my lovely family for encouraging me throughout my academic education. Without the inspiration, drive, and support of my parents and my sister, I might not be the person I am today. You are always there for me. Last but not least, I would like to thank my crazy friends all around the world for sharing great time and for the long talks during the difficult time of my studies. I'm glad to have you all by my side. Thank you.

Contents

List of Figures

List of Tables

List of abbreviations

CRDS	Cavity ring-down spectroscopy
DIC	Dissolved inorganic carbon
DO	Dissolved oxygen
DOC	Dissolved organic carbon
GPP	Gross primary production
NDIR	Non-dispersive infrared
NEP	Net ecosystem production
P	Production
POC	Particulate organic carbon
R	Respiration

1. Introduction

1.1 Carbon Cycle

Carbon is a fundamental building block of life because living organisms are composed of carbon-based molecules (Schulze-Makuch and Irwin, 2004). The carbon cycle is the biogeochemical cycle by which carbon is transferred and circulated between biosphere, hydrosphere, lithosphere and atmosphere. The fluxes within the carbon cycle can be fast or slow and each of the components of the earth system can act as a carbon source or sink. The fast domain of the global carbon cycle describes exchange fluxes between atmosphere, ocean and biosphere with rapid reservoir turnover times (from a few years to millennia). The slow component of the carbon cycle involves the huge carbon stores in rocks and sediments with slow reservoir turnover times (from 10,000 years to million years) (Ciais et al., 2013).

Before the industrial revolution and during the last 2000 years, the fast- and slow-carbon cycles maintained a relatively steady concentration of carbon in the atmosphere, land and ocean (Riebek, 2011). Since the beginning of industrial era, humans have altered the carbon cycle and the carbon dioxide (CO2) concentration in the atmosphere has increased almost by 90% (Ciais et al., 2013). Atmospheric CO2 with a current concentration of 400ppm (NOAA) represents the main atmospheric carbon species and is the most significant gas, after water vapour, for the greenhouse effect (Ciais et al., 2013). Between 1750 and 2011 the total anthropogenic CO2 emissions to the atmosphere were 555 PgC (Ciais et al., 2013). The major source of anthropogenic CO2 emissions to the atmosphere is burning of fossil fuels and cement production (Boden et al., 2011) as well as by changes in land use (deforestation) which causes a net reduction in land carbon storage (Ciais et al., 2013). However, not all of the carbon emitted by human activities has remained in the atmosphere due to uptake by the biosphere and the ocean. About half of these emissions stayed in the atmosphere 240 PgC and the rest is stored in the ocean (155

PgC) and in land (160 PgC) (Ciais et al., 2013). Figure 1.1 illustrates the exchange fluxes between atmosphere and other reservoirs in the fast component of the global carbon cycle. Black numbers represent the natural system for the time before the industrial era and red numbers represent carbon storage and annual anthropogenic fluxes during the time period 2000-2009.

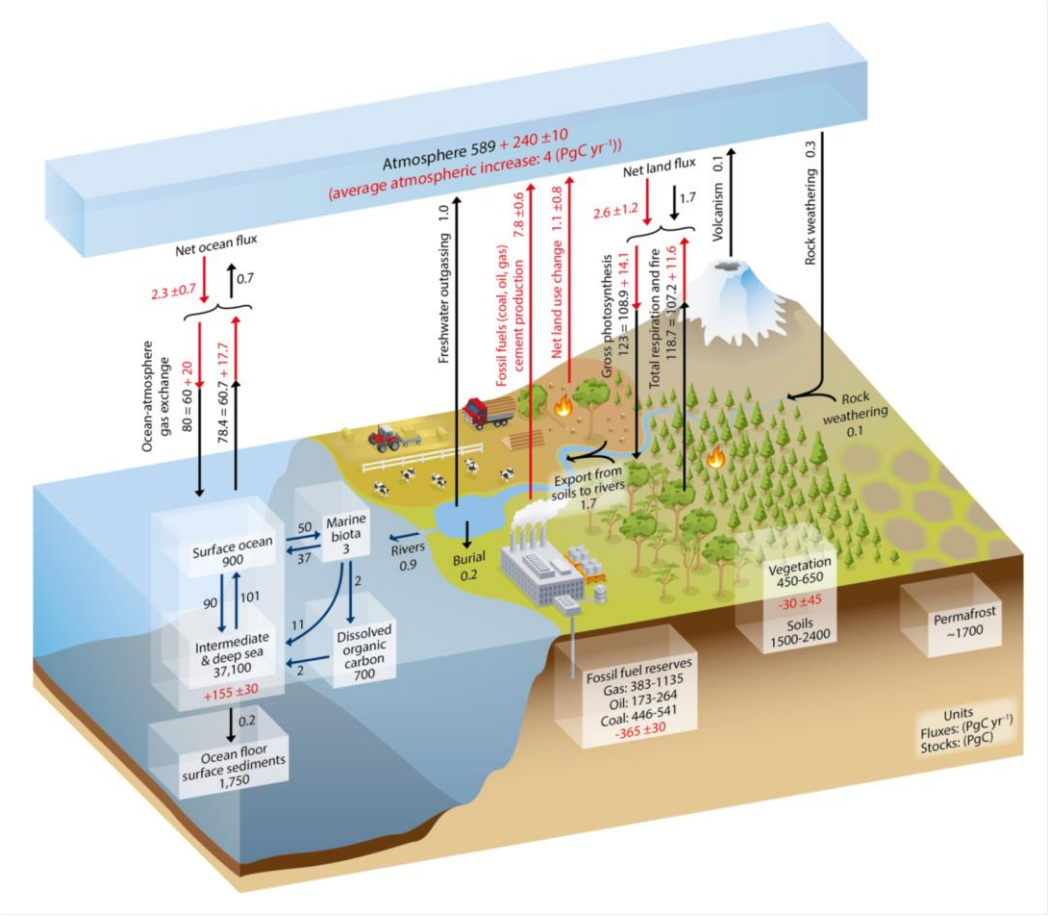

Figure 1.1: Global carbon cycle, numbers represent reservoirs in PgC and annual carbon exchange fluxes in PgC y^{-1} (IPCC, Ch6, 2013).

Atmospheric carbon exchanges with the terrestrial and marine biosphere by photosynthesis or with the hydrosphere by gas exchange or with lithosphere by chemical weathering and erosion (Riebek, 2011). Understanding the carbon cycle is thus vital to understanding present global climate change.

1.2 Role of rivers in the carbon cycle

Inland waters cover about 1% of the Earth's surface and only 0.1% of this area corresponds to rivers (Battin et al., 2009, Richey et al., 2002). Although this limited area rivers are of high importance for the global carbon cycle (Hope et al., 1994,

Aufdenkampe et al., 2011, Bianchi and Bauer, 2011). When the carbon enters inland waters, it can either be transported to the ocean, stored in sediments or escape to the atmosphere (Benstead and Leigh, 2012). Rivers and other inland waters can also be locations of intense carbon transformation. The two main processes were carbon is transformed are production and respiration.

A study of Cole et.al. (2007) estimated that inland waters receive 1.9Pg C y^{-1} from terrestrial landscape, of which approximately 0.7Pg C y^{-1} is emitted to the atmosphere via gas exchange, 0.2 Pg C y^{-1} is deposited in sediments and the remaining 0.9 Pg C y^{-1} is discharged to the ocean (Figure 1.2). However other studies by Raymond et al. (2013) estimate that streams and rivers emit as much as 1.8 GtC y^{-1} as CO_2. A more recent estimation excluding low stream orders revealed that emissions are reduced to 0.65 PgC y^{-1} (Lauerwald et al., 2015).

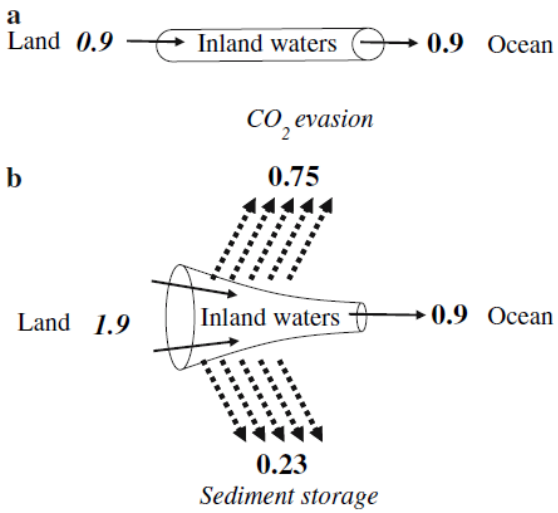

Figure 1.2: Schematic view of the role of inland waters to carbon cycle, passive pipe a, active pipe b, units (Pg C y^{-1}) (Cole et al., 2007).

1.3 Mass-balance equation

The mass balance equation for carbon reads (Cole et al., 2007).

$$I = G + S + E \quad (1.1),$$

where I is the total carbon of terrestrial origin imported to aquatic systems, G is the net carbon flux (outgassing), S is storage in sediments, and E is the export to the ocean. If the carbon input I is equal to the export to the sea E, then the rivers can be characterized as neutral passive pipes. In this case no transformation of carbon has

taken place in rivers and all the carbon is delivered to the ocean (Figure 1.2a). When the input of carbon I is larger than the export to the sea E, then a part of the carbon must be either stored in sediments or released to the atmosphere. In that case, inland waters are active components of the global carbon cycle and can be characterized as active pipes (Figure 1.2b). Recent research has shown that the passive pipe hypothesis is untenable, and that rivers contribute significantly both to carbon storage in sediments and to the transformation of carbon to gaseous species, which are ultimately released to the atmosphere (Regnier et al., 2013).

2. Theoretical Background

2.1 Carbon input to aquatic systems

Carbon enters inland waters from several pathways and in different chemical forms. Carbon is fractionated into two categories: inorganic carbon (IC) and organic carbon (OC). The major pathway for carbon input to aquatic systems is import from soils (organic and inorganic form) and chemical weathering of rocks (inorganic form).

2.1.1 Inorganic Form

Dissolved inorganic carbon (DIC) includes dissolved CO_2 , bicarbonate (HCO_3^-) and carbonate (CO_3^{2-}).

$$DIC = [CO_2]+[HCO_3^-] + [CO_3^{2-}] \quad (2.1)$$

Most inorganic carbon is transported as HCO_3^- and originates from weathering reactions such as the dissolution of carbonate minerals in sedimentary rocks (Hope et al., 1994). Bicarbonate and carbonate control the alkalinity of the inland waters. The total alkalinity is defined as "*The number of moles of hydrogen ion equivalent to the excess of proton acceptors (bases) over proton donors (acids) in one kilogram of sample*" (Dickson and Goyet, 1994). Dissolved CO_2 consists of aqueous CO_2 and carbonic acid (H_2CO_3) (Zeebe and Wolf-Gradrow, 2001),

$$[CO_2] = [CO_2 (aq)]+[H_2CO_3] \quad (2.2)$$

which is the solution of CO_2 in water according to the following chemical formula:

$$CO_2 + H_2O \rightleftharpoons H_2CO_3 \quad (2.3)$$

These two forms (CO_2 (aq), H_2CO_3), react as one in all chemical reactions in water and originate from the decomposition of soil organic matter, chemical weathering or gas exchange (Cole and Prairie, 2009).
In thermodynamic equilibrium, dissolved CO_2 and gaseous CO_2 are related ($CO_2(g) \rightleftharpoons [CO_2]$) according to Henry's law

$$[CO_2] = K_O\,(T,S)\cdot pCO_2 \quad (2.4)$$

Where $K_O(T,S)$ represents the temperature-salinity dependent Henry's law constant and pCO_2 the partial pressure of CO_2 in the gas phase.
The carbonate species according to Zeebe and Wolf-Gradrow (2001) are related by the following equilibria:

$$CO_2 + H_2O \rightleftharpoons HCO_3^- + H^+ \rightleftharpoons CO_3^{2-} + 2\,H^+ \quad (2.5)$$

For a fixed amount of DIC, the relative concentration of individual forms of inorganic carbon depends on the pH and the alkalinity of the water. In most freshwaters, DIC ranges from 10^{-4} mol L^{-1} in acidic soft waters to 10^{-3} mol L^{-1} in alkaline hard waters. In acidic waters, CO_2 is the most abundant constituent, while in natural waters, HCO_3^- is more abundant. The Bjerrum's plot (Figure 2.1) shows the relationship of the concentration of the three chemical species of DIC with pH. For example, at pH<6 most DIC is in form of CO_2, at pH 6.3 CO_2 and HCO_3^- are in equal quantities, while for 6.3<pH<10 the most abundant species is HCO_3^-. Finally, at pH>10 (basic water) the dominant present chemical species is CO_3^{2-}.

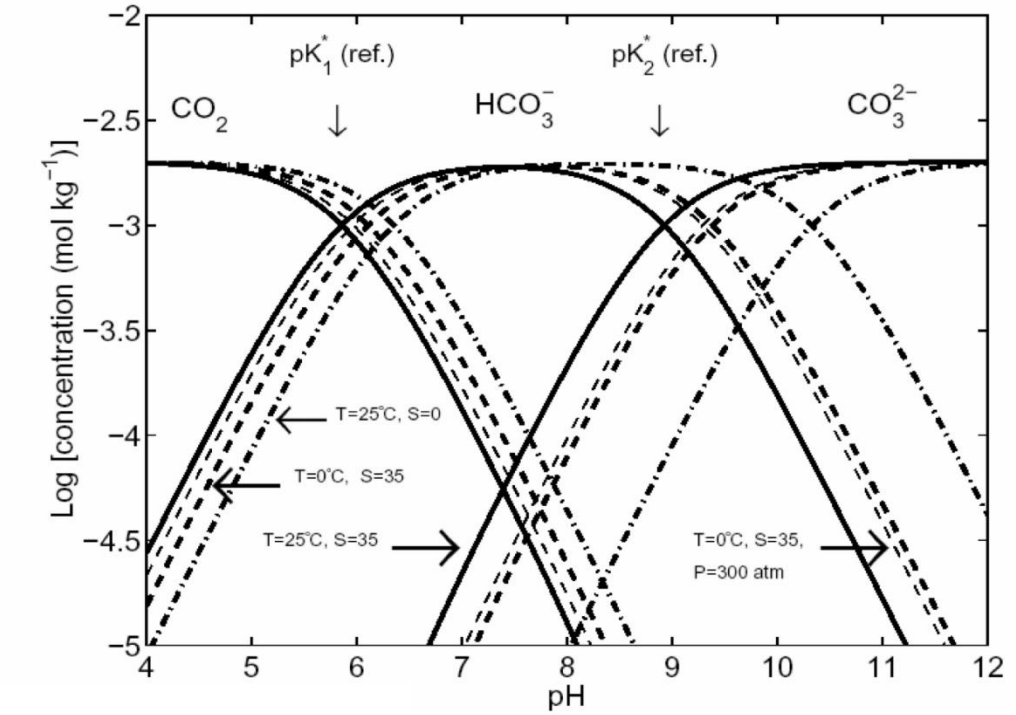

Figure 2.1: Bjerrum Plot, concentrations of DIC depending on pH, Zeebe and Wolf-Gradow, 2001

2.1.2 Organic Form

Organic carbon originates from vegetation and soil material as well as in-situ production of organic matter (Likens, 2010). The organic fraction of carbon that enters freshwater systems can either be dissolved organic carbon (DOC) or particulate organic carbon (POC). The two are distinguished by size; what passes through a filter with a pore size of 0.45 µm is classified as DOC, while the rest constitutes POC (Thurman, 1985) (Figure 2.2).

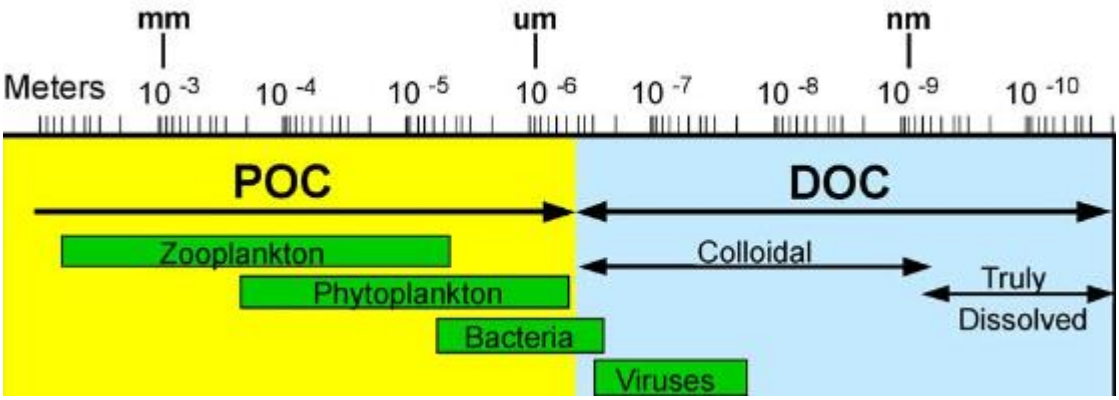

Figure 2.2: Size continuum spectrum of organic carbon, Verdugo et al., 2004

Approximately half of the organic carbon that enters inland water is transported to the ocean while the rest is oxidized within the system or stored in sediments in the form of POC (Hope et al., 1994) due to gravitational and drag forces. POC can remain in sediments for a long period of time but fresh and labile POC that is not stored can be transformed quickly (Prairie and Cole, 2009). POC can be transformed into DOC according to several process such as dissolution and enzymatic processes.

DOC is the most important intermediate in global carbon cycling because it can interact with microbes and be transformed rapidly producing CO_2. It is transferred with water and originates from the incomplete decomposition of soil and terrestrial plant material (Likens, 2010). On a global scale the pool of DOC is of the same magnitude as atmospheric CO_2 and accounts for approximately 20% of the organic material on the globe (Hopkinson et al., 2002). DOC is a highly complex mixture of compounds that are poorly chemically characterized (Koehler, 2012) and the knowledge for the composition and turnover of it is rudimentary for any aquatic systems (Hopkinson et al., 2002). Some studies classify distinct DOC pools according to the bioavailability of the different constituents and the turnover spans timescales of minutes to millennia (Koehler et al., 2012). The three distinct DOC pools with respect to their reactivity towards heterotrophic bacteria are labile, semi-labile and refractory DOC. Labile DOC is found in surface waters and is consumed in minutes to days, semi-labile DOC is found in deeper layers and has a turnover time of weeks to years and lastly refractory DOC mainly in ocean (>1000m) has a turnover time of millenia (Anderson and Williams, 1999, Carlson, 2002).

Another limited pathway by which carbon enters inland waters is through the atmosphere by diffusion. This process occurs in eutrophic systems when the partial pressure of CO2 in the water is lower than that of atmosphere. Volatile organic compounds and other organic material carried by dust can also enter from the atmosphere. Despite the large interface of the atmosphere with water, the input of carbon through this pathway is not significant (Likens, 2010).

2.2. Carbon cycling in aquatic ecosystems

The transformation of carbon between different species plays an important role for the biology and dynamics of aquatic systems (Giorgio and Williams, 2005). This transformation can proceed from the inorganic to the organic form of carbon as in photosynthesis and vice versa as in respiration. For example, in case of photosynthesis, CO_2 is converted to organic matter and the amount of carbon fixed by photosynthetic organisms comprises the Gross Primary Production (GPP) (Bianchi and Bauer, 2011). In other words, primary production is the storage of energy in chemical bonds by reducing carbon dioxide to carbohydrate in the presence of light (Giorgio and Williams, 2005). On the other hand, total respiration (R) is the biological oxidation of organic matter to CO_2. The difference between GPP and R of an ecosystem is the Net Ecosystem Production (NEP) (Aufdenkampe et al., 2011). All these processes are linked according to the following chemical equation:

$$\begin{gathered} \text{Photosynthesis} \rightarrow \\ 106CO_2 + 16HNO_3 + H_3PO_4 + 122H_2O \leftrightarrow (CH_2O)_{106}H_3PO_4 + 138O_2 \quad (2.6) \\ \text{Respiration} \leftarrow \end{gathered}$$

2.2.1. Respiration

Respiration is a process during which carbon is mineralised, oxygen is consumed, and CO_2 is produced. Two main forms of respiration can be distinguished: Autotrophic and heterotrophic respiration (Figure 2.2).

Autotrophic respiration is linked to the metabolism of primary producers. This kind of respiration is connected to primary production and takes place at a time scale of minutes to hours. For instance, when the photosynthesis rate increases, almost simultaneously an increase in algal respiration is recorded (Bianchi and Bauer, 2011). **Heterotrophic respiration** is linked to consumption of organic matter by bacteria, zooplankton, and fungi. This component of respiration is affected by the quality of the organic matter (DOC, POC). Its response time relative to primary production is at the scale of hours (DOC) to weeks (respiration based on POC) (Bianchi and Bauer, 2011). While fresh, labile organic matter is respired quite

rapidly, recalcitrant organic matter derived from resuspended sediments and phytoplankton production can also support heterotrophic respiration (Figure 2.2). The organic matter that supports heterotrophic respiration can be allochthonous or autochthonous. The term allochthonous is used for the organic matter derived from the surrounding terrestrial ecosystem mostly in dissolved organic form. The term autochthonous describes organic matter that was produced within the system. Despite the fact that autotrophic respiration has a shorter response time than heterotrophic respiration, the latter is mostly responsible for the total respiration. Most soil bacteria are heterotrophic and get the carbon from organic compounds and their energy from aerobic respiration. In order to characterise a system as autotrophic or heterotrophic, the ratio of primary production (P) to respiration (R) must be measured. Autotrophic systems produce more organic matter through photosynthesis than they consume through respiration (P>R). Heterotrophic systems consume more organic matter through respiration than they produce through photosynthesis (P<R).

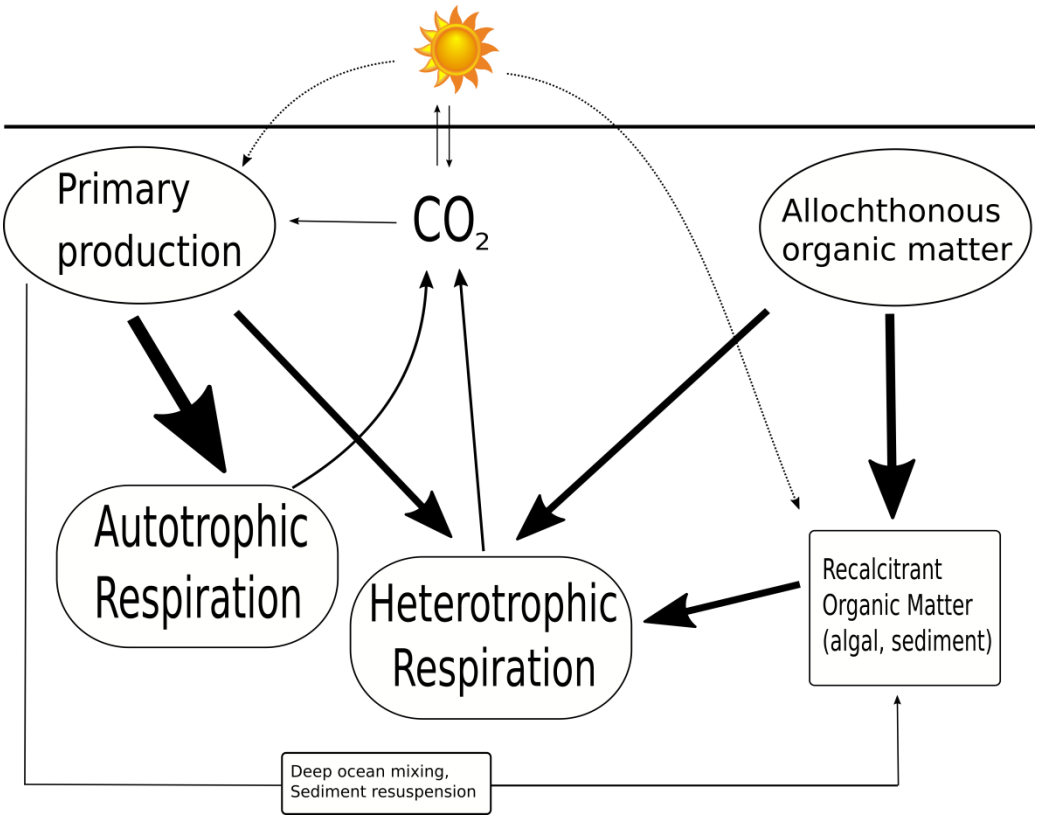

Figure 2.3: Main components of aquatic respiration, modified after Giorgio and Williams, Ch14. 2005

2.2.2 Decomposition

Respiration is a decomposition reaction. A decomposition reaction is the reverse of a combustion reaction such as photosynthesis. The major biochemical cycles that affected by decomposition are those of carbon (C), nitrogen (N), phosphorous (P), sulfur (S) and oxygen (O) (Wetzel et al, 1991). The decomposition of organic matter in aquatic ecosystems involves two processes; the hydrolytic degradation of high molecular weight organic polymers into compounds of low molecular weight (smaller particles), such as glucose, cellobiose and amino acids, and the nonhydrolytic oxidative mineralization of low molecular weight organic compounds like CO_2, H_2S and NH_4^+ (Wetzel et al.,1991).

The most common decomposition in nature is the aerobic decomposition. The aerobic process occurs when organic materials decompose in the presence of oxygen.

Organic compound + $O_2 \rightarrow CO_2 + H_2O$ + energy + Inorganic nutrients (2.7)

In a decomposition reaction the organic compound is oxidized by inorganic oxidizing agent (O,N,S etc.). In aerobic processes, O_2 is the oxidizing agent which gains the electron. The nutrients that formerly stored in organic form are mineralized during decomposition for use by living organisms (Wetzel et al., 1991). Carbon dioxide is produced and mostly escapes to atmosphere.

2.2.3 Rate of decomposition reaction

In order to understand the cycling of the carbon and the mechanism of aquatic ecosystems, one needs to be able to describe the decomposition kinetics and the biodegradability of organic matter. In situ measurements for determining the rates of organic matter decomposition is a difficult task. Decomposition is a continuous process, but the rate of decomposition varies with time depending on various substrate and environmental factors.

The relative rate of decomposition is related to various parameters according to (Wetzel et al., 1991)

$$k \propto \frac{T \cdot O \cdot N_u}{R \cdot S_p} \quad (2.8)$$

where T is temperature, O is dissolved oxygen or other electron acceptor, N_u are mineral nutrients responsible for microbial metabolism, R is the initial tissue refractivity and S_p is the particle size. Temperature is one of the most important factors regulating the speed of a decomposition reaction. Low temperatures slow the activity down, while warmer temperatures speed up decomposition. Despite of constant environmental and refractivity conditions the degradation of particulate organic matter can cause lower values of S_p and thus, increase the decay rates. The reaction rate of chemical reactions is the amount of a reactant reacted or the amount of a product formed per unit time. Often, the amount can be expressed in terms of concentrations and so the rate can be defined as

$$r = \frac{\Delta c}{\Delta t} \quad or \quad r = \frac{dc}{dt} \quad (2.9)$$

Where Δc is the change in concentration and Δt the time interval. When the rate vary with time and concentration we need to define the rate over a very small timescale using the derivative dc/dt. This fraction graphically represents the slope of the concentration against time.

The stoichiometry of the chemical reaction plays an important role so that the rate in case of a reaction

$$\mathrm{aA + bB \rightarrow cC + dD} \quad (2.10)$$

can be written as

$$\mathrm{r} = \frac{-1}{\mathrm{a}}\frac{\mathrm{d[A]}}{\mathrm{dt}} = \frac{-1}{\mathrm{b}}\frac{\mathrm{d[B]}}{\mathrm{dt}} = \frac{1}{\mathrm{c}}\frac{\mathrm{d[C]}}{\mathrm{dt}} = \frac{1}{\mathrm{d}}\frac{\mathrm{d[D]}}{\mathrm{dt}} \quad (2.11)$$

Negative signs are used for reactants and positive signs for products so that the rate is always positive.

The rate law is an expression relating the rate of a reaction to the concentrations of the chemical species present, which may include reactants, products, and catalysts. This rate can be calculated experimentally for the reaction 1 as

$$\text{rate} = k\,[A]^m[B]^n \quad (2.11)$$

k is the rate coefficient constant and m,n are the powers at which a particular concentration of each reactant is raised to. These powers describe the order of the reaction and in case of elementary reactions the orders are equal with the number of moles m =a and n =b. The orders do not have to be integers and the total order of the reaction is the summation of m and n (Atkins and De Paula, 2006).

2.2.4 Decay rates of dissolved organic carbon in inland waters

The decomposition rate which investigated in this study is the amount of organic carbon mineralized per unit time. If the overall process for the dissolved organic carbon decomposition reaction is :

$$DOC + O_2 \rightarrow CO_2 + H_2O \quad (2.12)$$

the rate, r can be calculated as

$$r = -\frac{d[DOC]}{dt} = -\frac{d[O_2]}{dt} = \frac{d[CO_2]}{dt} = \frac{d[H_2O]}{dt} \quad (2.13)$$

And the rate law for a second order reaction according to Equation 2.11 and 2.12

$$r = k \cdot [DOC] \cdot [O] \quad (2.14)$$

Whereas [DOC] accounts for the DOC concentration and [O] for the oxygen concentration.

Dissolved organic matter consists of numerous components with different biodegradability. Some of decomposition reactions that occur in aquatic systems are:

$$CH_2O + O_2 \rightarrow CO_2 + H_2O \text{ Formaldehyd} \quad (2.15)$$

$$C_6H_{12}O_6 + 6O_2 \rightarrow 6CO_2 + H_2O \text{ Glycose} \quad (2.16)$$

In the following the calculation for the decomposition rates are described when DOC decreases with time.

The simplest first order kinetic model which is applied in various studies (del Giorgio and Davies 2003) uses a single constant decay coefficient, k_1, which states that all component of organic matter decompose at the same rate so that

$$\frac{d[DOC](t)}{dt} = -k_1[DOC](t) \quad (2.17)$$

$$[DOC](t) = [DOC](t_0)e^{(-k_1(t-t_0))} \quad for\ t_0 = 0$$

$$[DOC](t) = [DOC](0)e^{(-k_1 t)} \quad (2.18)$$

where [DOC](t) is the concentration of DOC at a time t, [DOC](0) is the initial concentration of DOC at time t_0=0 and k_1 is the first order decay coefficient [units t^{-1}].

When DOC decreases with time then we expect that the change of CO_2 concentration with respect to time will be (Equation :

$$\frac{d[CO_2]}{dt} = -\frac{d[DOC](t)}{dt} = +k_1 \cdot [DOC](t) = k_1 \cdot [DOC](0)e^{(-k_1 t)} \quad (2.19)$$

$$[CO_2](t) - [CO_2](t_0) = -\frac{k_1}{k_1} \cdot [DOC](0)e^{(-k_1 t)} + \frac{k_1}{k_1} \cdot [DOC](0)e^{(-k_1 t_0)} (2.20)$$

$$[CO_2](t) = [CO_2](0) + [DOC](0) - [DOC](0)e^{(-k_1 t)} (2.21)$$

whereas $[CO_2](t)$ is the concentration of CO_2 at a time t, $[CO_2](0)$ is the initial concentration of CO_2 at t_0=0 and k_1 is the first order decay coefficient for the DOC change.

2.3 Ancillary parameters

2.3.1 Dissolved Oxygen

Dissolved Oxygen is the amount of gaseous oxygen (O_2) dissolved in the water. DO provide valuable information about the biological and biochemical reactions going on in waters and is one of the important environmental factors affecting the aquatic

life (Wetzel and Likens, 1991). Oxygen enters the water by direct interaction from the atmosphere, or as a by-product from plant photosynthesis. Water temperature and the volume of moving water can affect dissolved oxygen levels. Oxygen dissolves easier in cooler water than warmer water.

3. Motivation

Respiration is one of the two primary physiological processes in nature and the global respiration estimates for aquatic ecosystems are in the range of 170-200 Pg C y^{-1} (Giorgio and Williams, 2005). Despite the significant role of respiration in the global carbon cycle, most studies determine the CO_2 evasion from aquatic ecosystems without quantifying the processes that lead to these fluxes. Most rivers are a globally important source of CO_2 outgassing to the atmosphere (Cole et al., 2007, Aufdenkampe et al., 2011, Raymond et al., 2013, Lauerwald et al., 2015). Respiration of organic carbon is an important control on the CO_2 concentration in rivers (Richey et al., 2002). Other studies claim that lateral carbon inputs from surrounding soils and wetlands are more important than in-stream respiration (Borges et al., 2015). For a better determination of CO_2 fluxes and the transformation of carbon in aquatic systems, the processes that take place in the rivers must be examined. Among them, the most important process for CO_2 supersaturation is heterotrophic respiration. While there have been a number of decomposition studies conducted over the last years, decomposition rate constants were seldom reported (Hopkinson et al.,2002).

Thus, the goal of this study is to investigate the role of respiration for CO_2 outgassing from rivers. For this reason, the CO_2 concentrations from a tropical river in Malaysia and from Weser River in Germany will be quantified in a case study. The second part of this research is the development of an experimental setup that allows for the determination of respiration rates.

4. Experimental setup

4.1. Case study

4.1.1. Study area Rajang River

The Rajang River is the longest Malaysian river and is located in the northwestern part of the island of Borneo in Sarawak State. The Rajang River originates in the Iran Mountains, is 530 km long, and discharges into the South China Sea (Encyclopædia Britannica, 1998). The climate in Sarawak is tropical with high rainfall during the northeastern monsoon from November to February and less rainfall during southwest monsoon from March to October (Malaysian meteorogical department). The Rajang River drainage basin is about 50,000 km^2 in area (Staub et al., 2000) and flows through tropical rainforests, peat swamp forests and urban areas. The Rajang River delta plain covers 6,500 km^2 and peat (>3m thick) covers almost the half of the delta-plain region (Staub and Gastaldo, 2003). Due to deforestation, land use and high precipitation the Rajang River peat deposits have slightly extended (Gastaldo, 2010). Peat contains more than 65 % organic matter and peat soils represent a globally relevant major stock of soil carbon (Strack, 2008). Rivers that flow through these peatlands typically exhibit a black water colour, low oxygen concentrations, low pH values and small amounts of nutrients (Wetlands International –Malaysia, 2010).

Different authors (Baum et al., 2007, Moore et al., 2011, Müller et al., 2015) found that tropical peat draining rivers in Southeast Asia have exceptionally high DOC concentrations, resulting in a high lateral carbon flux. Therefore, the Rajang River is a large contributor of DOC to the South China Sea, exporting approximately 3.9 TgC annually (Müller-Dum et al., 2017).

4.1.2. Methods and instruments

pCO_2, DOC and POC concentrations in the Rajang River were determined during a measurement campaign on the Rajang River in August 2016. The methods and instruments used are briefly described in the following.

The underway measurements were taken from the boat SeaWonder and the setup is shown in Figure 3.1.

Figure 4.1: Picture of the research boat with accompanying instruments.

4.1.2.1. Weiss equilibrator

In order to determine the content of dissolved CO_2 in the surface water, an equilibrium between liquid phase and gas phase must be established. For this purpose, a Weiss equilibrator was used (Figure 3.2). A Weiss equilibrator consists of a chamber containing air at atmospheric pressure (Johnson, 1999). Surface water was pumped to the top of equilibrator at a rate of approximately 15 L min^{-1} creating a rapid equilibrium between water and air in the equilibrator (Dickson et al., 2007). The gas partial pressure was measured by a gas analyser connected in a closed loop with the equilibrator.

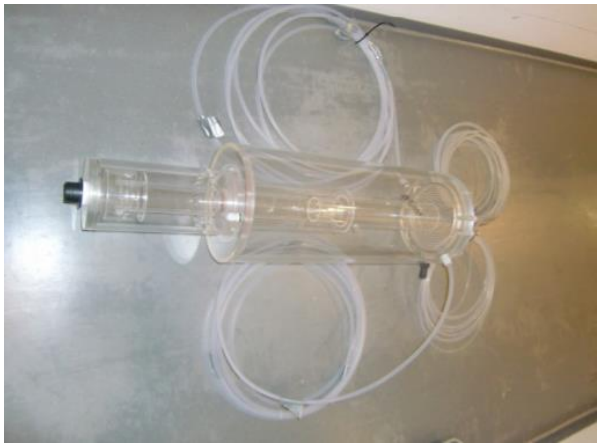

Figure 4.2: Picture of Weiss equilibrator.

4.1.2.2. LI-COR Gas Analyser

The CO_2 mole fraction was measured with a Non-Dispersive InfraRed (NDIR) analyser (Li-820, Figure 3.3). The Li-820 gas analyser is based on an infrared absorption detection system along an optical path. Sample air is continuously pumped through a 14 cm optical bench. An Infrared source emits radiation through this optical bench which interacts with the sample air. The CO_2 measurement is retrieved from the difference between a reference and sample signal recorded in the detector (LICOR, 2002). The two signals arise from the use of two narrow band optical filters, one of which captures the CO_2 absorption (centre at 4.24 μm wavelength), and the other one serves as reference (centre at 3.95 μm), where no CO_2 absorption occurs. Data output is recorded in a digital format after the instrument performs temperature and pressure corrections (LICOR, 2002).

Figure 4.3: Picture of the Li-820, NDIR gas analyser.

Before entering the gas analyser, sample air has to be dried in order to reduce H_2O absorption and to protect the electronics of the instrument. This is done by using a cartridge filled with magnesium perchlorate $Mg(ClO_4)_2$. For the calibration of the instrument three gas mixtures were used (500 ppm, 2000 ppm, 3500 ppm of CO_2), which were calibrated to the WMO reference scale by the Max Planck Institute for Biogeochemistry in Jena, Germany.

4.1.3. Ancillary measurements

In order to gain an understanding of the biological activities in the water, some additional physical and chemical properties of the water such as oxygen content, pH and conductivity were measured. **Dissolved oxygen** (DO) was continuously measured by an optical FDO 925 oxygen sensor with a WTW 3430 multi data logger. The sensor measures the concentration of oxygen in the sample water in mg L^{-1}. Since the concentration of the individual DIC are pH-dependent (see Section 2.1.1.), **pH** was measured at the stations using a SenTix 940 pH sensor. The K_o parameter in equation 2.7 is **temperature** and **salinity** dependent. In order to calculate the flux of gases, both parameters have to be quantified. Conductivity (as measure of salinity) was measured in µS cm^{-1} using a TetraCon925 conductivity sensor and temperature in ℃ using a WTW 3430 data logger (Xylem Inc., USA).

4.1.4. Water samples

During the campaign, water samples were taken at 34 stations from roughly 1 m depth in order to perform measurements of DOC, POC, as well as carbon and nitrogen isotopes ($\delta^{13}C_{org}$, $\delta^{15}N$). DOC samples were filtered through a 0.45 µm cellulose acetate filter before filling the water into bottles. The samples were acidified with phosphoric acid (H_3PO_4) and stored in a freezer. Analysis for DOC was performed by high temperature combustion using a TOC-VCSH analyser (Shimadzu, Japan). For the determination of POC, water samples were collected and filtered through pre-weighed and pre-combusted glass fibre filters. After the determination of the net sample weight, inorganic carbon was removed by addition of hydrochloric acid (HCl), and carbon and nitrogen contents were determined using flash combustion (EURO EA3000 Elemental Analyser, Eurovector, Italy). Isotopes were determined by mass spectroscopy (Finnigan Delta Plus, Thermo Fischer Scientific, USA).

4.2. Laboratory experiment

In order to study the role of respiration in the carbon cycle, two laboratory respiration experiments were performed. This section introduces the experimental setup and describes the methods and instruments which were used.

4.2.1. Setup

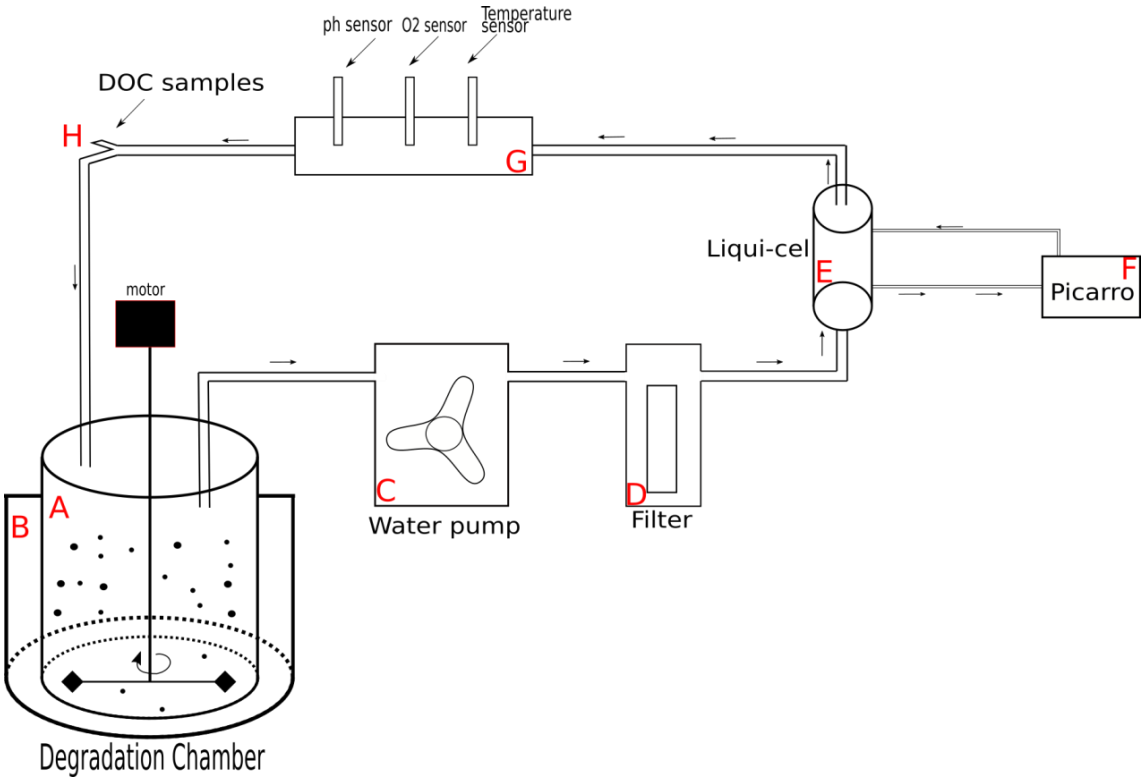

Figure 4.4: Schematic drawing of the experimental setup. Errors indicate the water flow.

River water respiration was studied with the experimental setup which is shown in Figure 3.4. Water for the experiment was taken from the Weser River in Bremen, and filled into the degradation chamber (Fig 3.4, A). A continuous stirring device was installed on top of the chamber to keep the water and the sediment well mixed. The upper part of the chamber (5-10 %) was filled with atmospheric air, to simulate natural river surface conditions. Water was circulated through the experimental set-up in a closed loop using a peristaltic pump and silicon tubes (Fig 3.4, C). The water

first passed a filter with fine pore size (Fig 3.4, D) to remove sediments before entering an equilibration device (Liqui-cel (Fig 3.4, E)). The CO2 partial pressure of the water was quantified by use of a gas spectrometer analyser (Picarro, Fig 3.4, F), which was connected in a closed loop to the Liqui-cel using PTFE Teflon tubing. After the Liqui-cel, the water passed through a cylinder with three sensors measuring auxiliary parameters before returning back to the degradation chamber. Additionally, a valve (Fig 3.4, H) enabled the sampling of water without interrupting the water flow.

Because respiration is a temperature dependent process, the water temperature was kept constant. For this purpose, an outer chamber was filled with water, which was thermostatted by a cooling device. All experiments were performed at the Leibniz Centre for Tropical Marine Research (ZMT).

4.2.2. Methods – Instruments

4.2.2.1. Liqui-cel

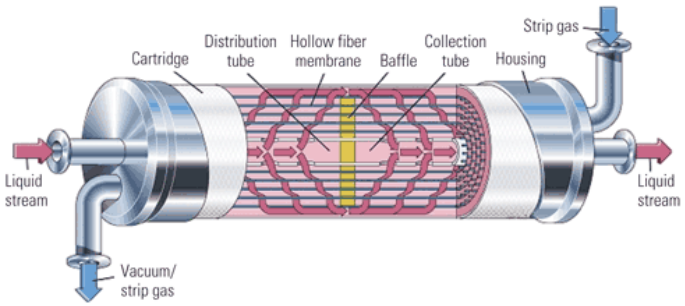

Figure 4.5: Schematic view of the Liqui-Cel.

In order to create an equilibrium between water and gas phase, a Liqui-Cel membrane contactor was used (Figure 3.5). This contactor contains thousands of microporous polypropylene hollow fibres around a centre tube. Since the hollow fibre membrane is hydrophobic, liquids will not penetrate the membrane pores. The water flows through the inside part of the hollow fibre and the gas on the outside in the opposite direction. This way, an equilibrium is established between the dissolved CO_2 in the water and the gas stream. The gas is circulated through the Picarro gas analyser for analysis (Wiesler and Sodaro, 1996).

4.2.2.2. Picarro

The CO_2 concentration was determined using a Picarro analyser, which is based on Cavity Ring-Down Spectroscopy (CRDS). The difference of CRDS with other spectroscopy analysers is in precision and sensitivity as CRDS uses an effective pathlength of many kilometres in a cavity. This long pathlength is due to three high reflectivity mirrors, which produce a continuous traveling light wave. A beam from a laser diode enters the cavity and because of reflection the cavity is quickly filled with light. After multiple reflections the light intensity decays to zero and the time needed for this ring-down is measured by a photodetector in terms of reflectivity of mirrors. Whenever a gas species that absorbs the laser light is inserted into the cavity, the ring-down time is accelerated. Calculating and comparing the ring-down time of the cavity with and without the absorbing gas species, gives the concentration of the target gas species.

4.2.3. Auxiliary parameters

During this laboratory experiment a series of physical and chemical properties of water were quantified. DO concentration, pH-value and temperature were measured continuously. The technical details of the sensors used were the same as during the underway measurements (see section 3.2.3.).

4.3.4. Water samples

Water samples were taken during the two experiments for DOC determination. All the procedure of collecting the samples and processing was exactly the same as during the underway measurements (see section 4.2.4).

5. Results and Discussion

This chapter presents the results and discussion of the described field work and experiments. In section 5.1 data from the tropical river in Malaysia are presented and discussed. In section 5.2 the results of the laboratory experiments are described and an improvement for future experiments is suggested. Finally in section 5.3 the focus lies on the Weser River in Germany and results of this study are compared to the laboratory experiments.

5.1 Field study in Malaysia

The focus of this section is on the field study performed in the Rajang river in Malaysia. Two measurement campaigns have been performed in 2016: one during the northeastern monsoon in January 2016 and one at the end of the dry season in August 2016.

5.1.1 Measured parameters at the Rajang River

Different parameters from the peat draining Rajang River were measured during two campaigns in 2016. The first campaign was performed by Denise Müller-Dum in January 2016. The second campaign was performed by me in August 2016. The averaged measured values and their standard deviations from both campaigns are presented in Table 5.1.

Table 5. 1: Mean pCO_2, DO, DOC and POC values in the Rajang River for non-estuary regions. The uncertainty represents one standard deviation (1σ).

	pCO_2 (µatm)	**DO (µmol L^{-1})**	**DOC (µmol L^{-1})**	**POC (µmol L^{-1})**
January 2016	2916 ± 570	193.8 ± 6	1633 ± 500	241.6 ± 158
August 2016	2905 ± 400	190.6 ± 16	4758 ± 1817	91.66 ± 33

During the first campaign in January, measured partial CO_2 pressure ranged from 1000 µatm to 4500 µatm with a mean of 2916 µatm. Very similar values were recorded in August when the pCO_2 ranged from 900 µatm to 5000 µatm with a mean of 2905 µatm. During both seasons the highest pCO_2 values were detected near the city of Sibu (dark red areas in Figure 5.1) and the lowest values were observed in the estuary regions where the salinity was larger than 2 PSU (Practical salinity unit) (dark blue areas in Figure 5.1). During both campaigns, relatively low DO concentrations were recorded: an averaged value of 193 µmol L^{-1} and 191µmol L^{-1} was measured in January and August respectively. The DOC concentrations showed a strong seasonal variation and averaged 1633 µmol L^{-1} in January and 4758 µmol L^{-1} in August. The lowest concentrations were recorded in the estuary regions where freshwater mixes with saline water. In both campaigns the highest values were recorded next to the city of Sibu. POC concentrations averaged 242 µmol L^{-1} in January and 92 µmol L^{-1} in August.

Table 5.2: pH and temperature measurements in the Rajang river for non-estuary region. The uncertainty represents one standard deviation (1σ).

	pH	**T (°C)**
January 2016	6.7 ± 0.1	27.5 ±0.3
August 2016	6.8 ± 0.1	29.2 ± 0.9

Water temperatures were continuously measured and averaged 27.5 °C in January and 29.2 °C in August (Table 5.2). pH measurements were conducted only during the station measurements and averaged to similar values for January and August (Table 5.2).

Compared to study from Harun et al. (2014) who measured DOC concentrations at the non-peat draining Kinabatangan River (the second longest River in Malaysia), the Rajang river (longest River in Malaysia) has high DOC concentrations. Moreover, DOC concentrations in the Rajang River during the wet season were higher than values measured in six other Indonesian peat-draining rivers studied in Wit et al. (2015) and Rixen et al. (2016) (averaged DOC concentration between 300 µmol L^{-1} to 1900 µmol L^{-1}). Müller et al. (2015) reported similar DOC concentrations as found in this study in the peat-draining Maludam River in Malaysia (averaged DOC concentration between 3200 µmol L^{-1} to 6200 µmol L^{-1}).

The observed strong seasonal variability of DOC, with high values in August and low values in January (Table 5.1), can be explained by two mechanisms. Firstly, a mechanism proposed in a study of Rixen et al. (2016) states that an increased freshwater discharge can dilute the DOC concentration in the river, which occurs mainly during the wet season. Secondly, another possible mechanism for the high DOC inputs is the recently constructed dams in the upstream Rajang River. Because of these anthropogenic activities, parts of the forests are flooded and the decomposing organic forest soil will lead to higher DOC yields into the rivers. Unfortunately, the extent of these anthropogenic disturbances remains unknown. However, a combination of the two described mechanisms could explain why the DOC concentration in the dry season (August 2016) is almost 3 times higher than in the wet season (January 2016). Nevertheless, it is difficult to define which process is the most important and leads to such seasonal variations, as there are only two campaigns performed in the Rajang River so far.

In contrast to the observed seasonal variability, the DOC concentration showed a weak spatial variability. It is assumed that one of the main terrestrial carbon pools, the peatland areas, is the main source of DOC in the Southeast Asian rivers (Moore et al., 2010). However, in the Rajang river no strong difference between DOC values between peat and non-peat areas was found, indicating that peat is not the dominant source of DOC. The high DOC values, especially in non-peat areas, could be explained by anthropogenic disturbances.

POC values in the Rajang river were similar to values found in other studies in Southeast Asia. For instance, POC concentrations of 308 μmol L^{-1} in the wet season and 92 μmol L^{-1} in the dry season were measured by Le et al. (2017) in Vietnam. The highest values in the Rajang River were recorded in the wet season. One possible reason for this could be the heavy rainfall which transports large amount of POC from soil to rivers (Moore et al., 2011).

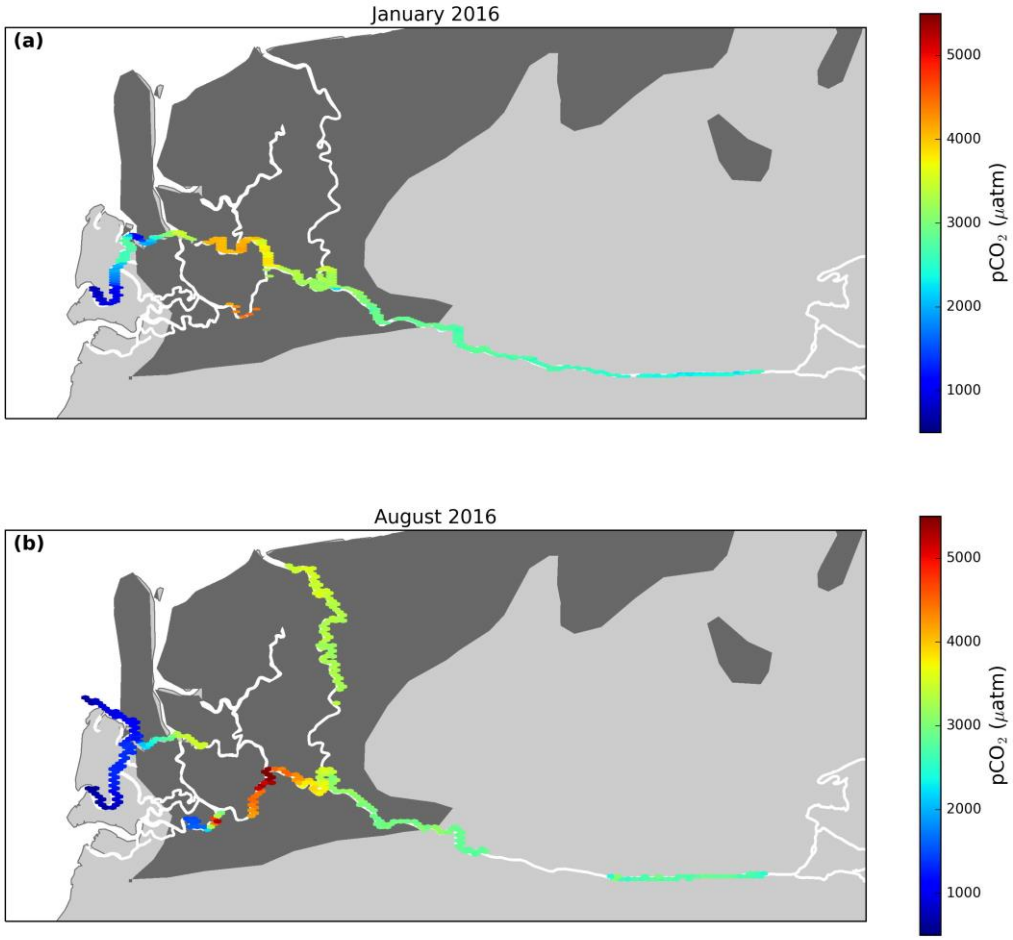

Figure 5.1: Spatial distribution of pCO_2 in the Rajang river (Müller-Dum et al., 2017)

The Rajang River was oversaturated with CO_2 with respect to atmosphere. Compared to a study performed by Wit et al. (2015) in different Southeast-Asian Rivers, low pCO_2 values were recorded in the Rajang river. The lack in seasonal variability in the pCO_2 measurements is consistent to what has been observed in other Malaysian Rivers (Müller et al., 2015). The significant higher pCO_2 values which were recorded in the peat areas, in comparison to the non-peat areas, indicate that peat pore waters are responsible for the enhanced pCO_2 values (Müller-Dum et al., 2017).

5.1.2 Correlation of pCO_2 and DOC

Figure 5.2 shows the correlation of pCO_2 to DOC for both campaigns. In both datasets, the pCO_2 and DOC were positively correlated. However, it was observed that for low DOC values the correlation was stronger than for higher DOC values. Especially in August, when the DOC exceeded 3500 µmol L^{-1} , lower CO_2 concentrations were observed, expected to be caused by a declining rate of CO_2 production due to limited in-steam respiration (Figure 5.2).

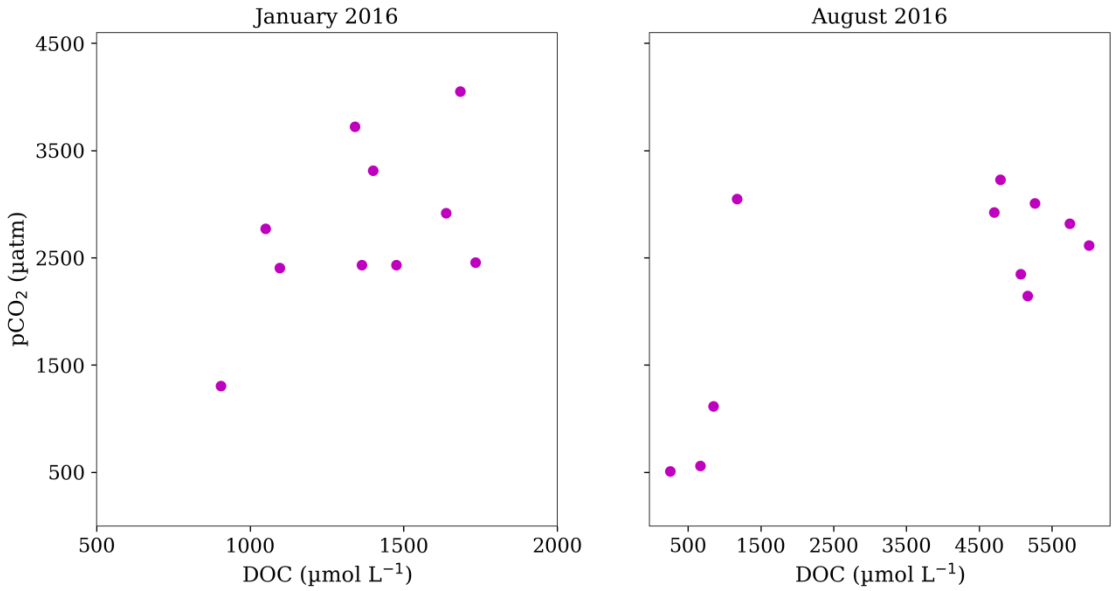

Figure 5.2 Correlation plots of DOC and pCO2 for both seasons.

Earlier studies have shown that high DOC concentrations lead to high pCO2 values (Wit et al., 2015). However, while very high DOC concentrations were observed in the Rajang River, only moderate pCO_2 values were recorded.

One possible explanation for this is that in areas where the DOC concentrations were more than 2000 µmol L^{-1}, also low pH values were recorded. According to a study of Wit et al., 2015 the acidic water limits the bacterial production which causes the DOC to decompose slower and the pCO_2 production to decrease. This indicates that, respiration in the Rajang River is not the dominant process for the CO_2 concentration.

Another explanation for this correlation is based on a study performed in a tropical African River, where it was proposed that the majority of CO_2 is derived from lateral inputs from wetlands and groundwater (Borges et al., 2015). We suggest that a similar mechanism is taking place in the Rajang River and expect that the DOC and pCO_2 are rather controlled by lateral input than by in-stream respiration (Müller-Dum et al., 2017). Concluding all the Rajang River appears to export the most DOC of its catchment to South China Sea.

5.2 Laboratory Experiment

In this section the focus is on the performed laboratory experiments. Two laboratory respiration experiments were performed at the Leibniz Centre for Tropical Marine Research (ZMT) in Bremen. The aim of these experiments was to study and measure the respiration rate and to determine how fast the different chemical substances taking part in the respiration reaction (Equation 2.12) interact with each other. Water samples for both experiments were taken from the Weser river in Bremen in January 2017. The location and the water sampling procedure were the same for both experiments and are therefore considered comparable. Directly after sampling the water was transferred to the laboratory and put into the experimental set up (described in section 4.2.1).

5.2.1 Measured parameters from experiments

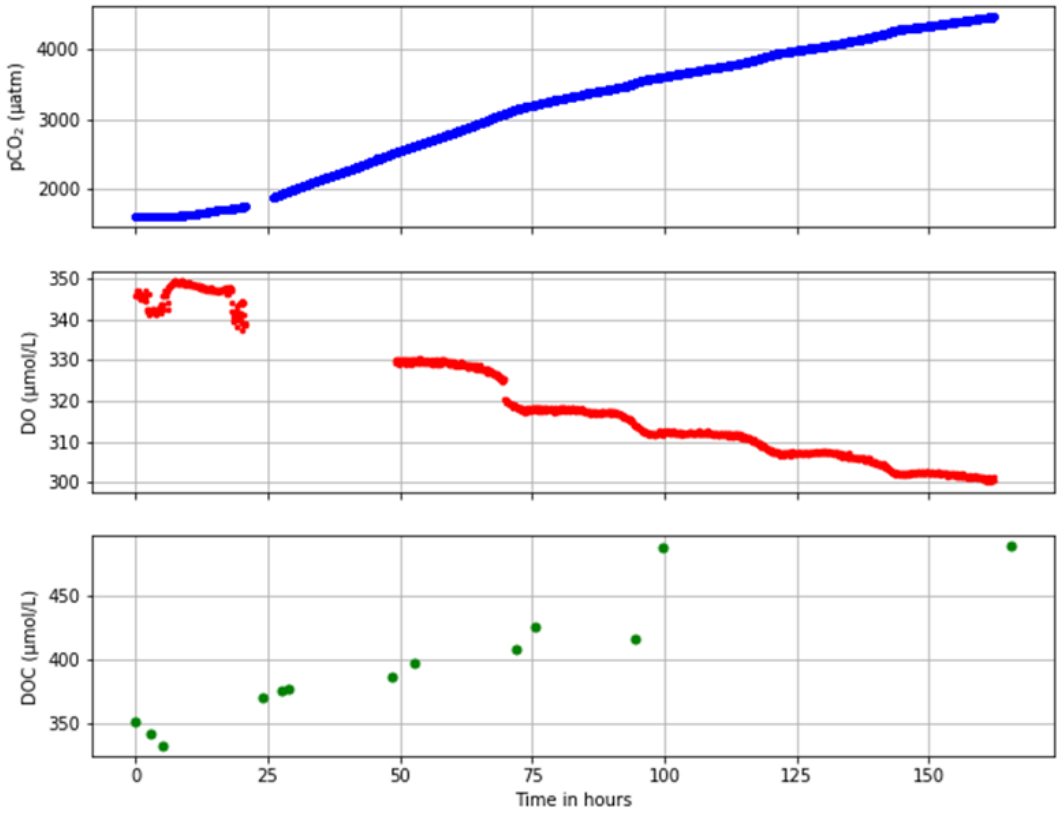

Figure 5.3: Measured pCO_2, DO and DOC values from the first experiment.

The first laboratory experiment was running for 162 hours. The obtained pCO_2, DO and DOC data from this experiment are shown in Figure 5.3. During the first

experiment, between the 20th and 26th hour, there was a leak in the experimental setup. Because a potential influence of atmospheric inflow cannot be excluded for this time period, the data from this period has been discarded. Moreover, due to a data storage failure, DO measurements from the 25th to the 47th hour are missing.

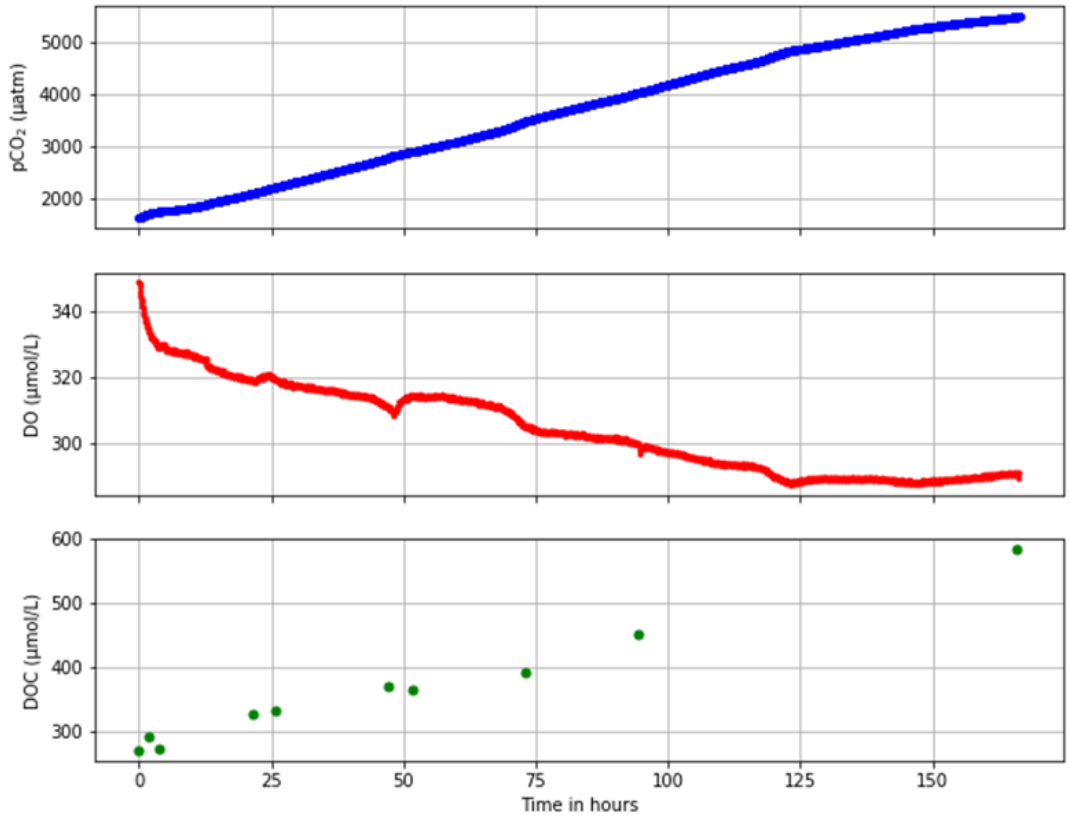

Figure 5.4 : Measured pCO_2, DOC and DO values from the second experiment

The second laboratory experiment was running for 166 hours. The pCO_2, DO and DOC data from the second experiment are illustrated in Figure 5.4.
For both experiments between the 100th hour until 160th hour no measurements of DOC were possible because the experiment was not accessible over the weekend.

In order to specify the magnitude of all variables, the mean and the median values of each experiment and parameter were calculated (Table 5.3). The uncertainty values are based on one standard deviation (1σ). During the first experiment, the partial pressure of CO_2 ranged between 1612 µatm and 4476 µatm, with a mean of 3172 µatm. During the second experiment, values ranged from 1722 µatm to 5490 µatm, with a mean of 3658 µatm (Table 5.3). The lower values were recorded at the beginning of each experiment and the higher values at the end of each experiment.

DO values ranged from 300 µmol L^{-1} to 349 µmol L^{-1} with a mean of 318 µmol L^{-1} during the first experiment and from 287 µmol L^{-1} to 348 µmol L^{-1} with a mean of 304 µmol L^{-1} during the second experiment (Table 5.3). During both experiments the maximum values were recorded at the beginning and the minimum values at the end of the experiments.

The total organic carbon in freshwater systems is composed of DOC and POC. During the two laboratory experiments only the DOC content was measured. 14 DOC samples were analyzed for the first experiment and 12 DOC samples for the second experiment. For both experiments, the first DOC concentration measurement was conducted before the water sample entered the experimental setup. Measured DOC concentrations varied between 284 µmol L^{-1} and 489 µmol L^{-1} in the first experiment with a mean of 388 µmol L^{-1}, and between 258 µmol L^{-1} and 583 µmol L^{-1} with an average of 354 µmol L^{-1} during the second experiment (Table 5.3). For both experiments the minimum DOC values were recorded at the beginning of the experiment and the maximum at the end of the experiment.

Table 5.3: Mean, median, start and end values for DO, DOC and pCO_2 for the two laboratory experiments

		Mean	Median	Start	End
Ex1	**DO (µmol/l)**	318.41 ± 14.44	313.44	349.38	300.31
	DOC (µmol/l)	388.61± 54.20	381.25	284.20	489.40
	pCO_2 (µatm)	3172 ± 904	3346	1612	4476
Ex2	**DO (µmol/l)**	304.45 ± 13.26	302.81	348.44	287.81
	DOC (µmol/l)	354.73 ± 91.49	330.40	258.30	583.00
	pCO_2 (µatm)	3658 ± 1211	3700	1722	5490

Water temperature and pH values were measured continuously and the mean values for the two laboratory experiments are listed in Table 5.4. The shown uncertainty represents one standard deviation (1σ). As described earlier, the water temperature was kept constant with temperature controlled device and averaged 12.96 °C and 13.42 °C in the first and second experiment respectively. In order to identify the relative concentrations of each form of DIC the pH was measured and it averaged to 7.56 for the first experiment and to 7.16 for the second experiment. These values

correspond to natural waters where HCO_3^- is commonly the most abundant species (Figure 2.1).

Table 5.4: Mean values for pH and temperature during the two laboratory experiments

	Ex1	Ex2
pH	7.56 ± 0.12	7.16 ± 0.23
T(°C)	12.96 ± 0.25	13.42 ± 0.37

In a closed system during the decomposition of organic matter, oxygen is consumed and CO_2 is produced. This is confirmed from the results for both experiments. Observing the pCO_2 data one can see that for both experiments the dissolved CO_2 in the water, pCO_2 increases continuously with time. This is expected to be an outcome of the continuous respiration of DOC that occurs in the experimental setup during the experiment.

In order to calculate the respiration rate coefficient the total CO_2 amount which is produced by the respiration has to be known. However, since part of the produced CO_2 will be transformed into other DIC species (mainly HCO_3^-), it would be necessary to measure the total DIC. During this experiment measurements of DIC were not possible. However, recording the pH values enables the calculation of the DIC concentration.

As explained in section 2.1.1, the relative concentration of individual forms of the DIC depends on the pH. An increase in the CO_2 concentration leads to an increase in hydrogen ions concentration $[H^+]$ and thus the equilibrium which is established by the carbonate system is shifted towards a lower pH (Pörtner , 2008). As expected during both experiments the pH decreased but the recorded decrease did not completely correspond to the CO_2 production. There are several explanations for this discordance. Firstly, a DOC buffering system might be present, wherein organic carbon molecules in neutral waters absorb the released $[H^+]$ resulting in a relatively moderate pH decrease. For basic soils the $[H^+]$ absorption of DOC is stronger than for acidic soils (McCauley et al., 2017). Secondly, Schulz et al. (2005) performed a study determining the rate constants for the CO_2 to HCO_3^- inter-conversion and showed that there is a chemical disequilibrium caused by the relatively slow

chemical inter-conversion. This process sums up to the pH buffering, while the CO_2 concentration in the water sample continuously increases. For these reasons, a calculation of the total DIC is not possible in this study and therefore only the measured pCO_2 concentrations are used for the following calculations. It is assumed that the underestimation of the produced CO_2 is similar during the whole experiments.

During both experiments, the DOC data showed an unforeseen increase in DOC concentrations. The DOC and the CO_2 concentrations are closely linked through the process of organic matter decomposition and in a closed system, such as during the experimental respiration process, a consumption of organic matter is expected and thus a decrease in the DOC concentration. However, in this study the DOC concentration increased with time. This indicates that a process inside the experimental setup continuously produced DOC. The possibility that the system influenced by photosynthetic processes is excluded (dark conditions). A possible hypothesis for the continuous increase in DOC concentration is the potential breakdown of POC due to the continuous circulation of the water through the experimental setup. Another hypothesis is that the material of the tubes and of some parts of the experimental setup could release DOC. In order to be able to investigate the cause of this continuous DOC increase, the POC content of the water should be measured. Moreover, in order to test the possible contamination of all devices in the set up, a blank experiment is required. During the performed experiment, the suggested additional measurements were not possible since the experiments were conducted in an extrernal institution (ZMT), and due to the fact that the time was limited because the instruments had to be shipped to a different measurement campaign. For these reasons a method, as explained in Section 5.2.4, is developed to be able to interpret the observed increase in DOC.

The DO concentration showed a moderate decrease over time in both experiments nonetheless, water was oversaturated with oxygen. This ensures that the respiration process is not limited by absence of oxygen (anoxic conditions). A small variation in the DO concentration over time is observed and this can be explained by small temperature variations.

5.2.2 Correlation of pCO_2 and DOC

Figure 5.5 and 5.6 show the measured pCO_2 and DOC concentrations of the first and second experiment over time. A pCO_2 increase with increasing DOC is observed for both experiments. Red markers assign the DOC concentration and the blue line indicates the continuously measured pCO_2 values.

During the first experiment (Figure 5.5) pCO_2 and DOC are not increasing uniformly. Between hours 0 and the 90 the DOC and pCO_2 values both increase strongly. After the 90th hour the DOC concentration suddenly peaks to 480 µmol L^{-1} at the 100th hour and maintains this concentration until the end of experiment, while the pCO_2 remains its steady increase. A possible explanation for this could be the failure of the DOC concentration measurement at the 100th hour. Unfortunately, no other DOC measurements were taken between the 100th hour and the 160th hour because the experiment was running over the weekend.

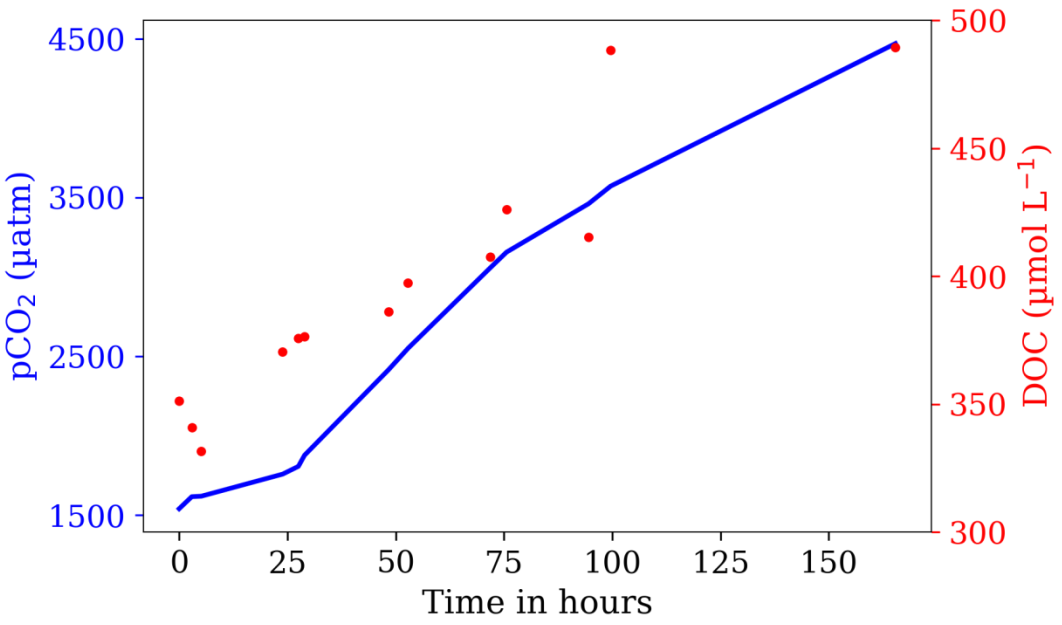

Figure 5.5 DOC and pCO_2 change over time during the first experiment

During the second experiment (Figure 5.6) the pCO_2 and DOC increase over time are showing a very similar rate and thus the DOC values do not diverge from the blue line which indicates the pCO_2 concentrations.

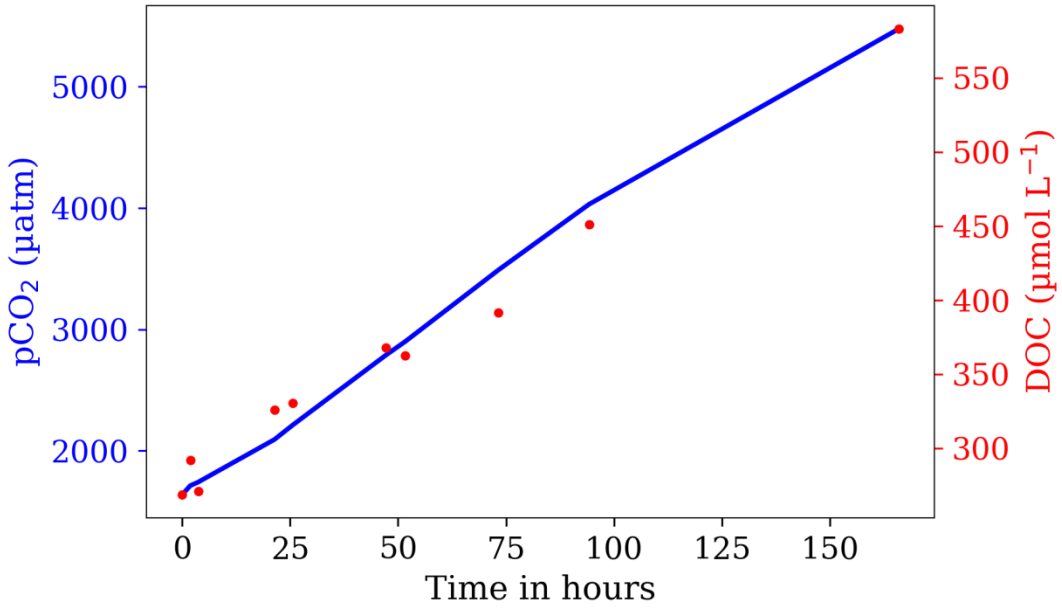

Figure 5.6 DOC and pCO_2 change over time during the second experiment

Figure 5.7 shows the correlation of CO_2 and DOC. A strongly positive correlation is observed between pCO_2 and DOC concentration during both experiments. For the first experiment the correlation coefficient of DOC with the pCO_2 is 0.94 and for the second experiment it is 0.98.

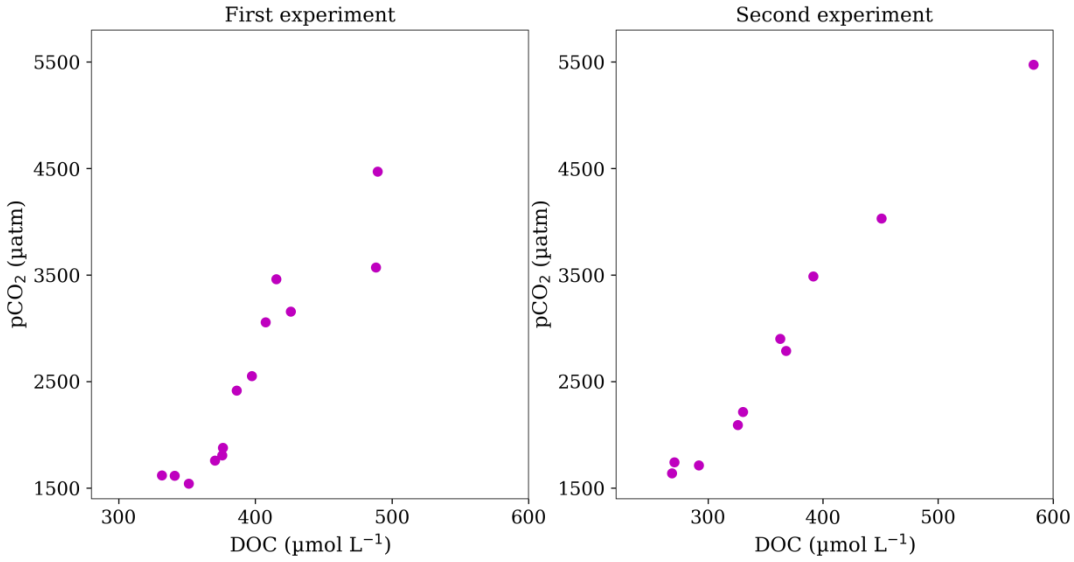

Figure 5.7 Correlation between DOC and pCO_2 for the two laboratory experiments.

5.2.3 Rate of change of pCO_2 and DO

In order to investigate the kinetics of organic matter decomposition the decomposition rates need to be calculated (see Equation 2.13). In the following the rate of change for pCO_2 and DO have been calculated.

It can be noticed that the partial pressure of CO_2 increased steadily for both experiments. To be able to determine the respiration rate from the pCO_2 value, the change of pCO_2 with respect to time was calculated by:

$$r_{pCO_2} = \frac{\Delta pCO_2}{\Delta t} \quad (5.1)$$

Linear regression over pCO_2 time series was used to determine the respiration rate. It was observed that this rate was solely positive as a result of the almost steady increases in pCO_2 during both experiments.

For the first experiment, firstly the rate for the whole experiment timespan was calculated to be 19.29 μatm h^{-1} (Figure 5.8a). Afterwards a more linear part of the curve was selected (from the 30th hour until the end of the experiment) which resulted in a calculated rate of 18.45 μatm h^{-1} (Figure 5.8b). Finally, two shorter time series were selected where the data points (blue colour in figure 5.8c-d) were observed to fit well to the fitted line (red line in Figure 5.8c-d) so that the calculation can be more precise. Between the 30th and 70th hour the rate was 26.91 μatm h^{-1}, and between the 80th and 160th hour the rate was observed to be smaller: 14.75 μatm h^{-1}.

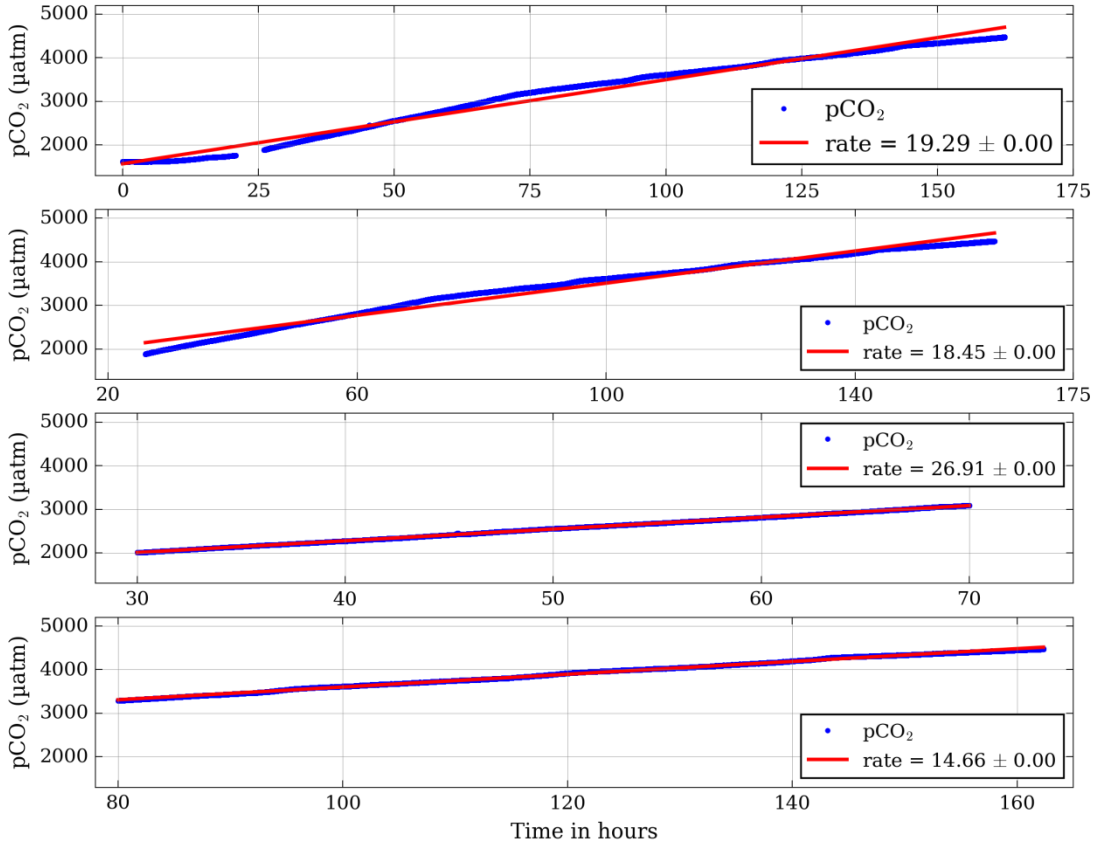

Figure 5.8 Rate of change of pCO_2 over time for the first experiment.

The same calculations were repeated for the second experiment. In this case, the calculated rate for the whole timespan was 24.91 µatm h^{-1}, and use of a shorter data selection (from 20th hour until the end of the experiment) resulted in a calculated rate of 24.79 µatm h^{-1} (Figure 5.9a-b). Again two shorter time series with the best linear fit were selected to be able to calculate more precise rates which resulted in 24.79 µatm h^{-1} (based on the 20th to the 100th hour) and in 20.67 µatm h^{-1} (based on the from 100th to the 160th h)(Figure 5.9 c-d).

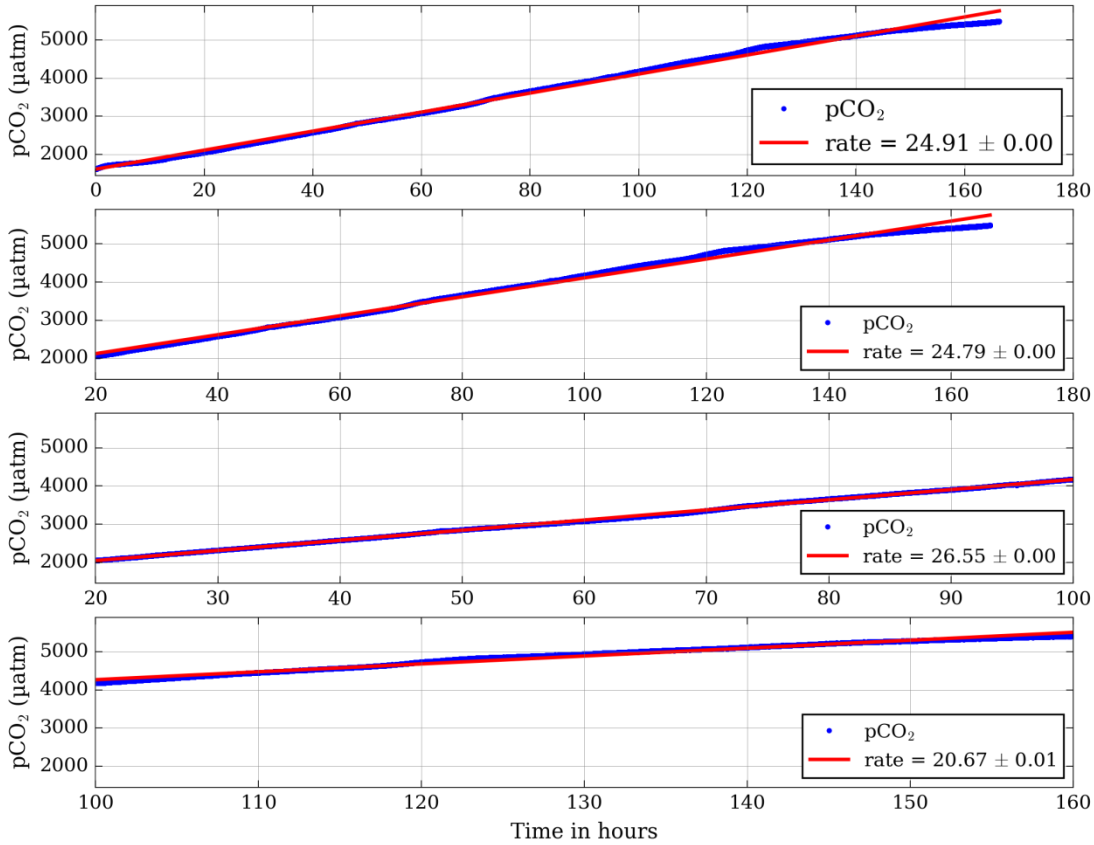

Figure 5.9 Rate of change of pCO_2 over time for the second experiment.

The same procedure as before was followed in order to determine the respiration rate from the DO concentration. Here the slope of the line represents the change of DO with respect to time.

$$r_{DO} = \frac{\Delta DO}{\Delta t} \qquad (5.2)$$

The rate for the whole timespan was calculated to be -0.31 µmol L^{-1} h^{-1} wherein the negative sign represents the observed decrease in DO concentration (Figure 5.10a). In order to be able to compare the change in pCO_2 with the change of DO with respect to time, the same time series selection should be done. For this reason, the rate from the 30th hour until the end was calculated to be -0.27 µmol L^{-1} h^{-1} (Figure 5.10b). For the time series of the 47th - 70th hour and the 80th - 160th hour, the rate was calculated to be -0.20 µmol L^{-1} h^{-1} and -0.23 µmol L^{-1} h^{-1} respectively (Figure 5.10c-d). The error of each rate was calculated and is shown in the legend of each plot: the longer the time series, the smaller the error of the rate.

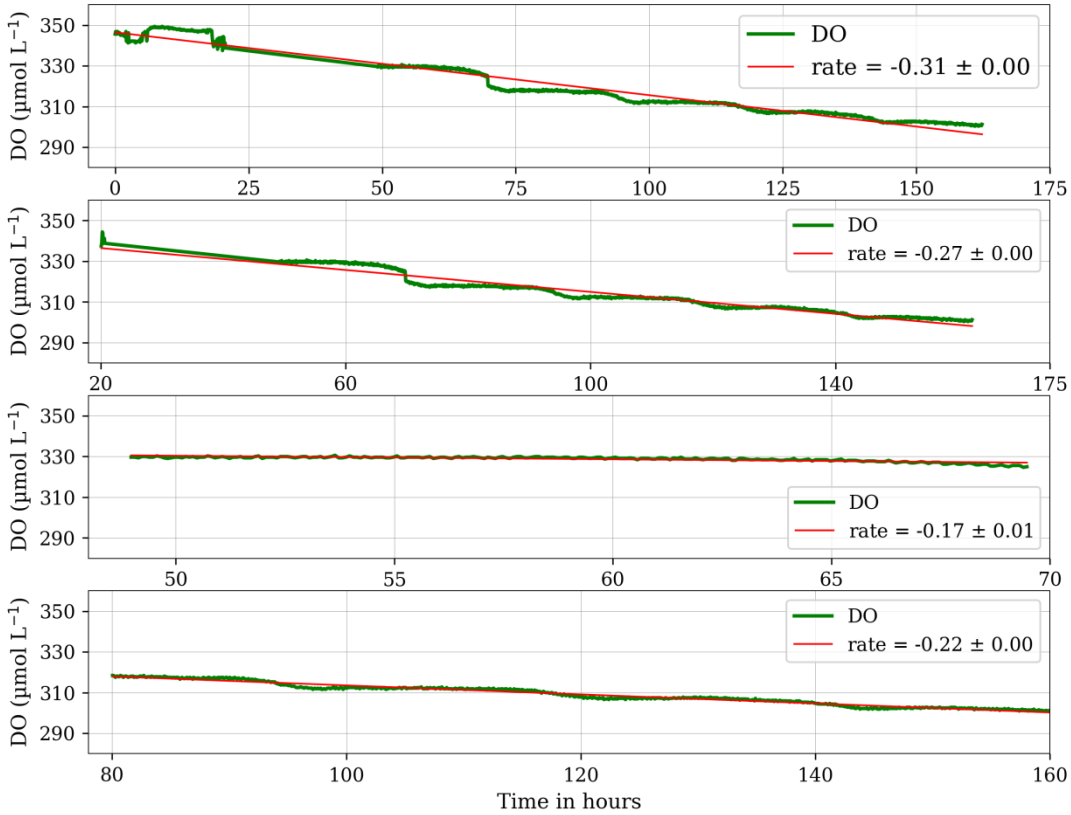

Figure 5.10 Rate of change of DO over time for the first experiment.

A moderate decrease of DO concentration was observed during the second experiment. Based on the best fitting lines, the calculated rates ranged from -0.21 µmol L^{-1} h^{-1} to -0.29 µmol L^{-1} h^{-1} (Figure 5.11c-d). The averaged rate for the whole timespan was -0.27 µmol/ L h^{-1} while, based on measurements from the 20th hour until the end, the rate was -0.25 µmol L^{-1} h^{-1} (Figure 5.11a-b).

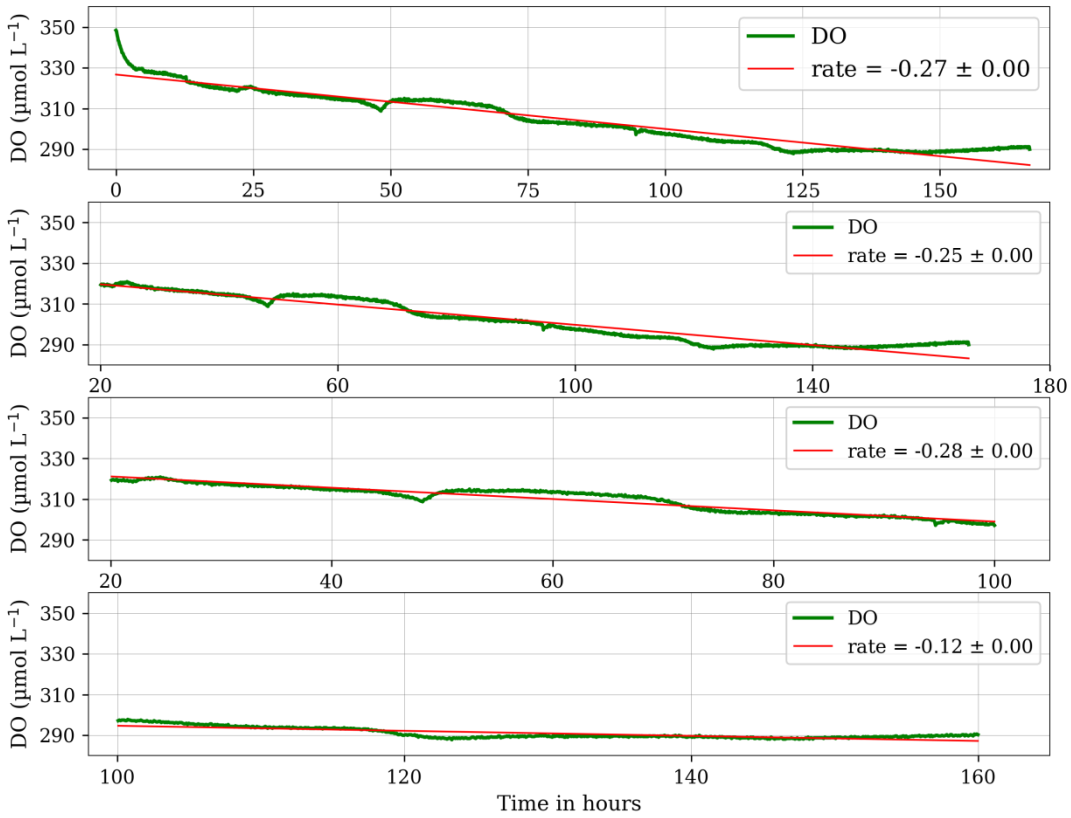

Figure 5.11 Rate of change of DO over time for the second experiment.

Based on the Equation 2.4, the dissolved CO_2 concentration in water has been calculated and, based on this value, the corresponding r_{CO_2}. Table 5.5 shows the measured CO_2 and DO for the selected time series.

Table 5.5: Calculated respiration rates for different time series for both experiments.

Variable	**1st experiment**			**2nd experiment**		
Time Series	total	30 - 70	80 - 160	total	20 - 100	100 - 160
CO_2 (µmol L^{-1} h^{-1})	0.94	1.15	0.63	1.21	1.13	0.88
DO (µmol L^{-1} h^{-1})	- 0.31	- 0.17	- 0.22	- 0.27	- 0.28	- 0.12

The total calculated rates for the two experiments are in not consistent. The calculated rate of CO_2 production for the second experiment is larger than the calculated rate of CO_2 for the first experiment. This difference can be explained by the higher DOC production rate which is calculated in the next section. If more DOC is added into the water, it can results to a larger decomposition rate. Moreover, it is observed that the calculated rate for CO_2 concentration is higher in

the beginning than at the end of both experiments. A similar behavior is observed for the calculated rate for the DO concentration only for the second experiment. Indeed a change in the rate of CO_2 production because the labile fraction of DOC is decomposed quicker than the semi-labile and more recalcitrant part. This is validated by a study performed by Pollard (2013) which states that the rate depends on the lability of the DOC. The more labile the DOC soil is, the quicker it will decompose.

For each experiment, a significant difference between the r_{CO_2} and r_{DO} is observed. A possible explanation for this discrepancy is that the DOC contains enough oxygen molecules to undergo respiration without a supplementary need from the water oxygen molecules in the sample. For this reason, the decrease in oxygen concentration is more moderate than that of the CO_2 concentration.

5.2.4 Rate of change of DOC

In order to calculate later the rate coefficient k of the decomposition reaction the continuous DOC concentration of the water sample is needed. For this reason a procedure is developed and described in this subsection.

The DOC concentration from the first experiment gently decreased over the first 8 hours and then grew from ~360 µmol L^{-1} in the 20th hour to ~500 µmol L^{-1} at the end of the experiment (Figure 5.10). The total increase was used to determine the slope of the linear fit. To be able to calculate the rate of change of DOC :

$$m = \frac{\Delta DOC}{\Delta t} \qquad (5.3)$$

The rate for the whole timespan was determined to be 1.08 µmol L^{-1} h^{-1} , and for the selected time series (30th - 80th hour) to be 0.96 µmol L^{-1} h^{-1} (Figure 5.12).

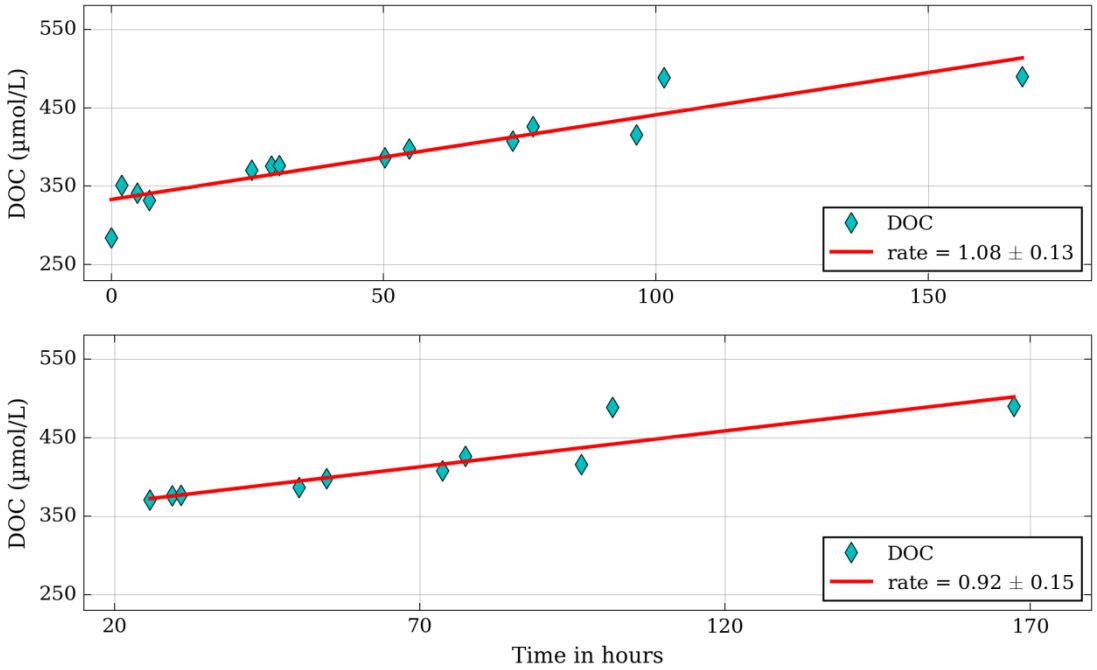

Figure 5.12 Rate of change of DOC over time for the first experiment.

The DOC concentrations during the second experiment showed similar behavior to the first experiment. During the first 10 hours, the concentration slowly decreased and for the rest of the period a moderate increase was recorded. Figure 5.6 illustrates the rate of this change to 1.85 µmol L^{-1} h^{-1} for the total period of the experiment and 1.80 µmol L^{-1} h^{-1} for a shorter time (Figure 5.13).

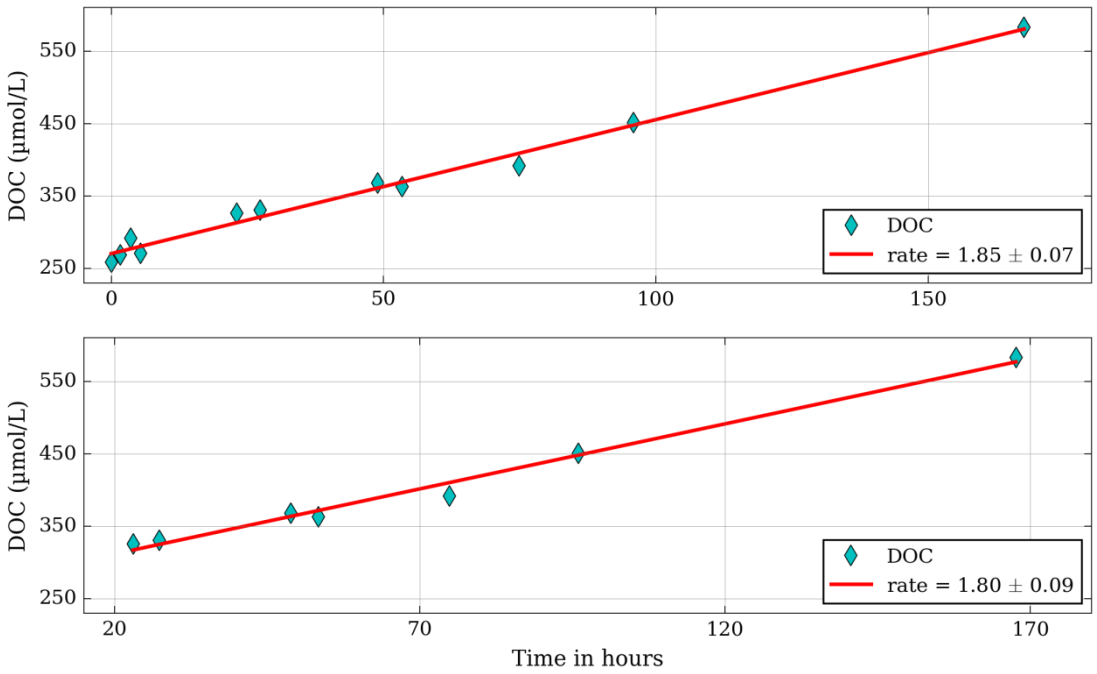

Figure 5.13 Rate of change of DOC over time for the second experiment

Comparing the two regression lines, the DOC measurements with their standard deviation of the second experiment fit better with the fitted line than the first experiment. For both experiments a linear relationship for the DOC over time is recorded which can be expresses by the formula:

$$[DOC](t) = a + m \cdot t \quad (5.4)$$

m is the slope of the linear increase and a is the y-axis intercept of the regression line which is close to the initial DOC concentration.

Alternatively equation 5.4 for the first experiment can be written as:

$$[DOC](t) = a + 1.08 \cdot t \quad (5.5)$$

And for the second

$$[DOC](t) = a + 1.85 \cdot t \quad (5.6).$$

The rate of change of DOC for the second experiment is larger by 70% than the rate of change for DOC for the first experiment.

5.2.5 Calculation of rate coefficient k

For this study the rate at which CO_2 concentration is produced can be written as (see Equation 2.13):

$$r = \frac{d[CO_2]}{dt} \quad (5.7)$$

Moreover, according to the rate law (see Section 2.2.3, Equation 2.11), the rate of the reaction of the DOC decomposition can be written as:

$$r = k \cdot [DOC] \cdot [O] \quad (5.8)$$

This calculation refers only to second order reactions and is an approximation for the calculation of the rate coefficients. Combing Equation 5.7 and 5.8 k can be expressed as:

$$k = \frac{d[CO_2]/dt}{[DOC]\cdot[O]} \quad (5.9)$$

As described before, during the experiments the DOC concentration increases linearly with time. According to that k will be :

$$k = \frac{d[CO_2]/dt}{[a+m\cdot t]\cdot[O](t)} \quad (5.10)$$

whereas *m* is the derivative of DOC with respect to time (Equation 5.3). For both experiments, the CO_2 concentration [CO_2] was calculated by converting the measured partial pressure of CO_2 to the molar concentration using the Henry's law (Equation 2.4).

The calculated mean k values $7.62 \cdot 10^{-6}$ μmol^{-1} L h^{-1} for the first experiment and $1.06 \cdot 10^{-5}$ μmol^{-1} L h^{-1} for the second (Table 5.5). In both experiments the calculated rates were based on the total length of the experiment. For the first experiment *m* was calculated to be 1.08 µmol L^{-1} h^{-1} while for the second experiment the calculated change was 1.85 µmol L^{-1} h^{-1}.

Table 5.6: Calculation of k rate coefficient

	1st experiment	2nd experiment
k [µmol^{-1} L h^{-1}]	$7.62 \cdot 10^{-6}$	$1.06 \cdot 10^{-5}$

The rate law can be written for the first experiment (Equation 5.6) and for the second experiment (Equation 5.7) as:

$$\frac{\mathrm{d}[CO_2]}{dt} = 7.62 \cdot 10^{-6} \cdot [DOC](t) \quad (5.6)$$

$$\frac{\mathrm{d}[CO_2]}{dt} = 1.06 \cdot 10^{-5} \cdot [DOC](t) \quad (5.7).$$

5.2.6 Recommendations for future experiments

Improvement of the experimental setup

The purpose of the setup was to measure respiration rates by monitoring the change in DOC and CO_2 concentrations. The following recommendations can improve a possible future experimental setup. First of all, the performance of a control experiment with purified water is essential to be able to investigate background effects. This control experiment will test the behavior of all individual parts of the experiment and will show whether specific materials will affect the experimental setup or the measurement of respiration rates. Secondly, as explained before, it is

important to completely remove the particulate organic carbon of the water sample. For this reason, the water sample should be filtered by a 0.45 μm cellulose filter before entering the experimental setup. Also, another parameter that can affect the respiration process is ambient light. Thus, it is necessary to ensure complete darkness to eliminate photoautotrophic organic carbon production. Lastly, the duration of each experiment should be extended until CO_2 concentration in the water reaches a plateau. Only then the decomposition of DOC for this water sample is completed and results represent a better performance of a respiration reaction.

Improvement of the monitoring of data

Additional measurements are required to identify the age of the dissolved organic carbon. Published studies (Hopkinson et al., 2002, Koehler et al., 2012) state that there is a strong connection between the age of organic carbon and its decomposability. Furthermore the turnover of DOC is largely determined by the bioavailability of the different constituents and thus some bacterial composition measurements will improve our understanding of the system. Calculation of bacterial growth should be conducted from the start of the incubation. Last but not least, DIC measurements will enable the authentication of the pH measurements.

5.3 Rates from Drakenburg Weser data

A combination of model experiments under laboratory conditions and field studies has the potential to expand the depth of understanding the respiration process in rivers. In this subsection, data from a measurement campaign at the Drakenburg station in Weser river, Germany will be shown and will be compared to the data from the laboratory experiment. The campaign was performed in October 2015 by members of the IUP group and DOC concentrations were taken from FGG-Weser Datenbank.

5.3.1 Measured parameters in Weser River

The pCO_2 and DO shows daily pattern, which is expected to be caused by photosynthesis and respiration. During the day, when there is solar radiation, photosynthesis is dominant and thus pCO_2 values decrease. During the night, respiration processes dominate and pCO_2 concentration values increase. As highlighted before, oxygen concentration are inversely correlated with CO_2 and therefore here also these variables vary inversely (Figure 5.14).

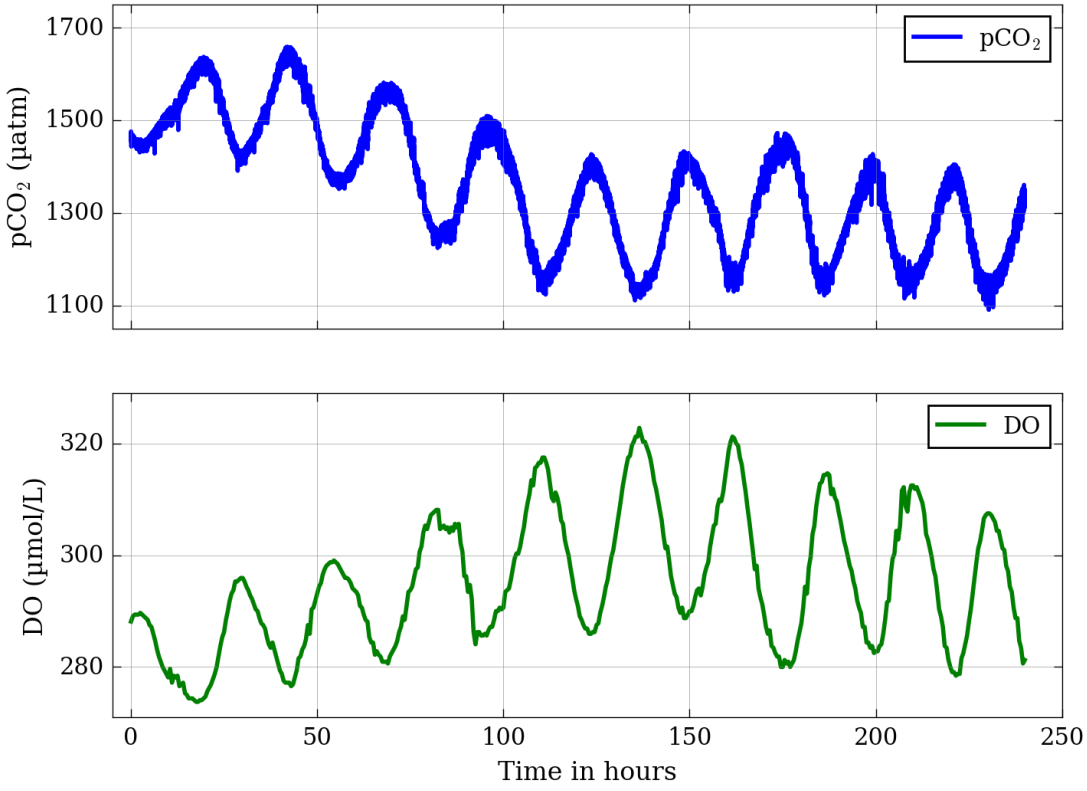

Figure 5.14: Daily variations of pCO_2 and DO concentrations at the Drakenburg monitoring station.

Table 5.7 presents the variables measured at the Drakenburg monitoring station. Mean values were calculated and the uncertainty represents one standard deviation (1σ).

Table 5.7 Mean values for pCO_2, DO, DOC, pH and T at the Drankenburg Weser station.

Variable	Mean
pCO_2 (µatm)	1361 ± 137
DO (µmol L^{-1})	295 ± 12
DOC (µmol L^{-1})	339 ± 52
pH	8.0 ± 0.2
T (°C)	15.5 ± 1.3

The DOC concentration of Weser River was quite similar to the DOC concentration of the water sample during the first 20 hours of the experiments. The conservative behavior of DOC is observed also in other estuaries and derives from simultaneous sources followed by minimal DOC turnover over time (Moran et al., 1999).

5.3.2 Rates from Drakenburg Weser data

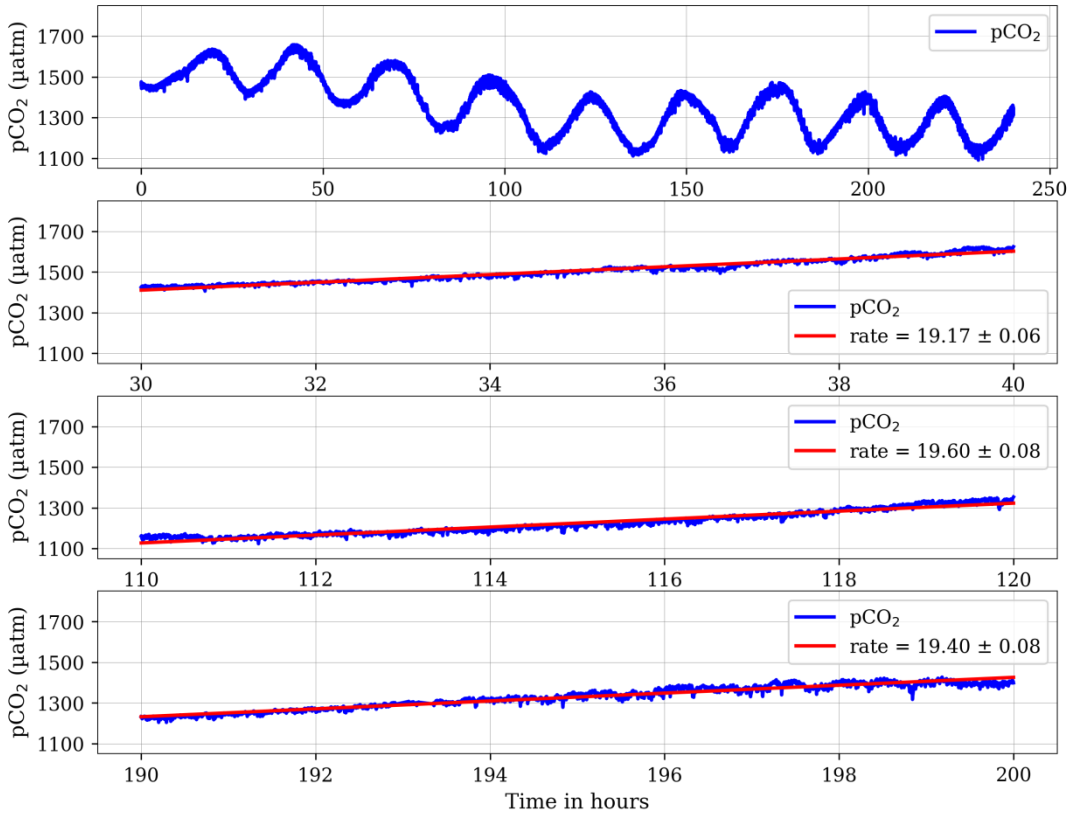

Figure 5.15: Rate of change of pCO_2 over time

For this study, only data during night were selected when the respiration process is dominant. In this case only a timespan of approximately 10 hours during the night could be selected to calculate the respiration rates. For the pCO2 change three shorter time series were selected: 30th - 40th h, 110th - 120th h and 190th - 200th h. The calculated rates ranged from 19.17 µatm h^{-1} to 19.60 µatm h^{-1} with an average of 19.39 µatm h^{-1} (Figure 5.15).

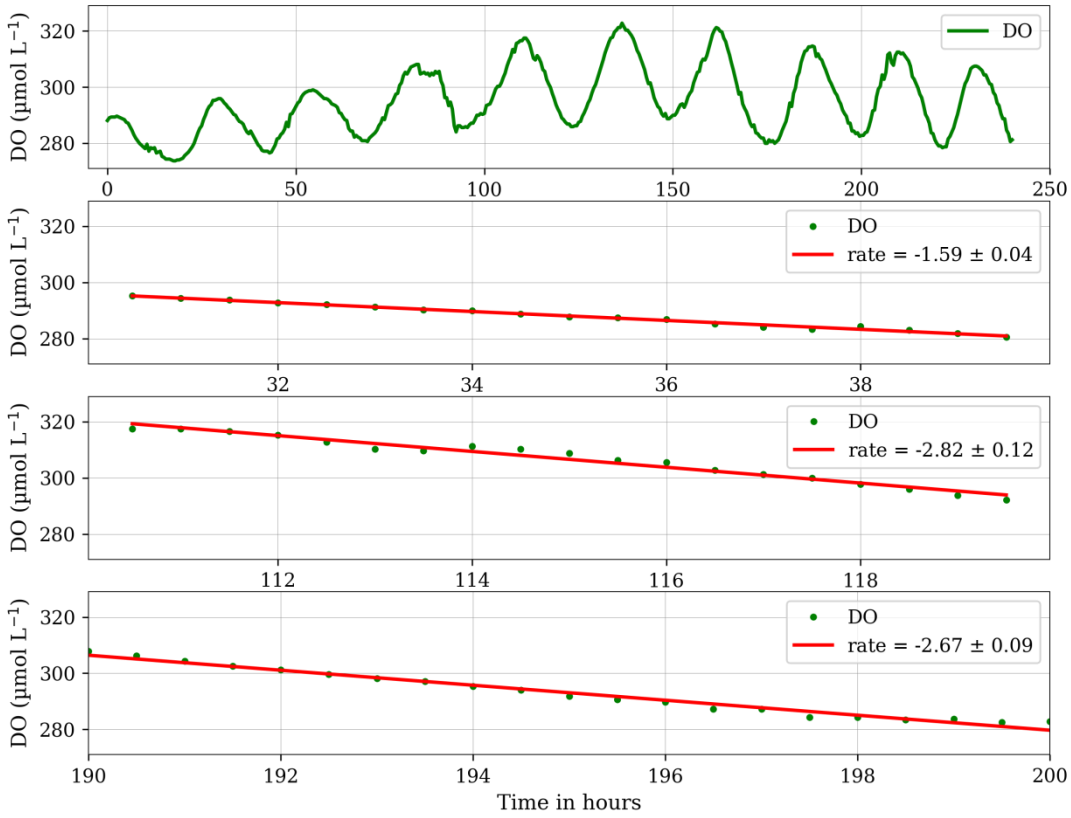

Figure 5.16: Rate of change of DO over time

The same procedure was implemented for the change of DO concentration with respect to time. The same time spans were selected for DO concentrations. The calculated rate ranged from -1.59 µmol L^{-1} h^{-1} to -2.82 µmol L^{-1} h^{-1} with an average of -2.36 µmol L^{-1} h^{-1}(Figure 5.16).

In the Weser River there is a constant supply of organic carbon within the river flow. Consequently, the DOC concentration is assumed to be constant over time at the Drakenburg station. The rate coefficient k can be calculated using the Equation 5.9

$$k = \frac{d[CO_2]/dt}{[DOC] \cdot [O]} \quad (5.9)$$

Whereas the $d[CO_2]/dt$ represents the mean rate of change of CO_2 over time which was calculated before, and converted to mole fraction via Henry's law (equation 2.4) using a K_o for 15.5 °C. For DOC concentrations the mean value was used which is presented in Table 5.7.

The resulting k rate coefficient is $8.79 \cdot 10^{-6}$ µmol L^{-1} h^{-1}. Therefore the rate law can be written as

$$\frac{d[CO_2]}{dt} = 8.79 \cdot 10^{-6} \cdot [DOC] \quad (5.10)$$

5.3.3 Comparison of the different rates and rate coefficients

Between different laboratory experiments and in-situ measurements, it is expected to find different calculated rates of CO_2 and DO concentrations since bacterial physiological states might be altered differently during the different sampling moments (Pollard, 2013).

Table 5.8: Mean calculated rates from the two laboratory experiments and from the Weser data.

Variable	1st exp	2nd exp	Weser
CO_2 (µmol L^{-1} h^{-1})	0.94	1.21	0.88
DO (µmol L^{-1} h^{-1})	- 0.31	- 0.27	- 2.35

The results in Table 5.8 indicate that, in the field experiment case study, the respiration rate defined from the rate of DO concentration is higher than in the experiment. This outcome is expected since many DOC might already respire in the first few minutes after sampling, which results in an unintentional manipulation of the experiment.

The calculated respiration rate of CO_2 is smaller in the field experiment case study than in the laboratory experiments. The hypothesis is suggested for this difference and is based on the difference in the CO_2 and O_2 fluxes between the surface water and the atmosphere. As the river water during the field measurements was

oversaturated with oxygen, a thermodynamic equilibrium was established and there was no net exchange of oxygen. On the other hand, the CO_2 concentration of the river water was a lot higher than that of the atmosphere. According to Fick's law and assuming that for 15 °C the exchange coefficient k is similar to both gases, an escape of CO_2 towards the atmosphere could be the reason for the lower calculated respiration rates defined from the change of CO_2 over time.

The results in Table 5.9 present all the calculated rate coefficients for the two laboratory experiments and from the field measurements in the Weser River. Although the experimental setup had several limitations, the calculated respiration rate coefficients are similar to those calculated based on the in-situ measurements.

Table 5.9: Mean calculated rate coefficients from the two laboratory experiments and from the Weser data.

	1^{st} experiment	2^{nd} experiment	Weser
k [μmol^{-1} L h^{-1}]	$7.62 \cdot 10^{-6}$	$1.06 \cdot 10^{-5}$	$8.79 \cdot 10^{-6}$

6. Conclusion

Carbon dynamics of inland waters are strongly related to the decomposition of organic matter. In this Master thesis, the role of respiration (decomposition) in rivers is investigated. Respiration is the transformation of organic matter to CO_2, performed by bacteria in the water column or in the sediment. During the decomposition of organic matter, oxygen is consumed and CO_2 is produced. Therefore, strong relationships between organic matter (DOC, POC), dissolved oxygen concentrations (DO) and partial pressure of CO_2 (pCO_2) are usually observed in aquatic ecosystems.

In this thesis, several aspects of the carbon cycle were studied and discussed. Firstly, a case study about carbon dynamics of the tropical Rajang River in Malaysia was presented. The second topic of the thesis was the development of a novel laboratory setup by use of an incubation chamber. The set up was tested and its possible use for the determination of river water respiration rates was evaluated. Finally, the thesis shows the comparison of the calculated respiration rates from the laboratory experiment with the continuous in-situ respiration measurements in the Weser River.

Results from two different field campaigns at the tropical Rajang River (Malaysia) were evaluated, of which one took place in the wet season and one in the dry season. The Rajang River is characterized by the presence of peatlands in the delta region (~11 % of the catchment area) and by human activities (deforestation and damming) in the non-peat areas on the upstream in its catchment. In comparison to other non-peat draining rivers, high DOC concentrations were recorded. DOC concentrations were in consistence with other peat-draining rivers in Southeast Asia. No strong difference in DOC values was found between peat and non-peat areas, indicating that peat is not the dominant source of DOC. The presence of anthropogenic disturbances is one possible reason for the observed high DOC concentration in the upper part of the river. Also, a strong difference between campaigns was observed (DOC averaged 1633 μmol L^{-1} in the wet season and 4758 μmol L^{-1} in the dry season). A hypothesis for this high annual variability is that,

during the wet season (heavy rain) the river becomes relatively diluted. Also the recently constructed dams could have an effect on the annual behaviour of the DOC concentrations.

Despite the high DOC concentrations, the recorded pCO_2 concentrations in the Rajang River were relatively moderate averaging to 2916 µatm in the wet season and to 2905 µatm in the dry season. This indicates that only a very small fraction of the organic matter in the Rajang River respires and is returned to the atmosphere, and that most of the DOC is exported to the South China Sea. This confirms the hypothesis that DOC and pCO_2 in the Rajang River were rather controlled by lateral inputs (anthropogenic disturbances) than by in-stream processes and by the presence of peatlands in the catchment. To what extent the anthropogenic activities influence the carbon dynamics of inland waters still has to be investigated.

In the second topic of this Master thesis, the laboratory experimental setup was tested for two water samples from the Weser River and measurements of DOC, DO and CO_2 concentration were conducted. An unexpected increase of DOC was recorded during the respiration process and different hypotheses for this phenomenon have been described (degradation of particulate organic carbon, release of DOC from the instrumental parts). Furthermore, a new method has been developed to calculate respiration rates which accounts for this DOC increase. The limitations of the experiment and its accompanying conclusions were evaluated and possible improvements for future experiments have been formulated.

The last part of this study focuses on the comparison of respiration rates from the laboratory experiment with continuous in-situ measurements at the Drakenburg station in the Weser River. The results indicate that the respiration rates in the in-situ measurements are higher than in the laboratory experiment. It is likely that the most labile fraction of organic matter in the river water decomposes in the first few minutes right after sampling, and so before the start of measurements, which might explain the difference in the calculation of the respiration rates. This bias might explain the difference in the calculation of the respiration rates. Nevertheless, the calculated rate coefficients from laboratory experiments ($7.62 \cdot 10^{-6}$ µmol L^{-1} h^{-1} for

the first water sample, $1.06 \cdot 10^{-5}$ µmol L^{-1} h^{-1} for the second water sample) are similar to the in-situ measurements ($8.79 \cdot 10^{-6}$ µmol L^{-1} h^{-1}).

List of references

Anderson, T. R., and Williams P. J. (1999). A one-dimensional model of dissolved organic carbon cycling in the water column incorporating combined biological-photochemical decomposition. Global Biogeochemical Cycles, 13(2), 337–349.

Atkins, P. W., & De, P. J. (2006). Atkins' Physical chemistry. Oxford: Oxford University Press.

Aufdenkampe, A. K., Mayorga, E., Raymond, P. A., Melack, J. M., Doney, S. C., Alin, S. R., Aalto R.E. and Yoo, K. (2011). Riverine coupling of biogeochemical cycles between land, oceans, and atmosphere. Frontiers in Ecology and the Environment, 9(1), 53-60.

Battin, T. J., S. Luyssaert, L. A. Kaplan, A. K. Aufdenkampe, A. Richter, and L. J. Tranvik (2009). The boundless carbon cycle. Nature Geoscience 2:598-600.

Baum, A., Rixen, T., and Samiaji, J. (2007). Relevance of peat draining rivers in central Sumatra for the riverine input of dissolved organic carbon into the ocean. Estuarine, Coastal and Shelf Science, 73(3), 563-570.

Benstead, J. P., and Leigh, D. S. (2012). An expanded role for river networks. Nature Geoscience, 5(10), 678-679.

Bianchi, T. S., and Bauer, J. E. (2011). 5.03 Particulate Organic Carbon Cycling and Transformation. Treatise on Estuarine and Coastal Science. Academic Press, Waltham, 69-117.

Boden, T.A., G. Marland, and R.J. Andres. (2011). Global, Regional, and National Fossil-Fuel CO_2 Emissions. Carbon Dioxide Information Analysis Centre, Oak Ridge National Laboratory, U.S. Department of Energy, Oak Ridge, Tenn., U.S.A.

Borges, A. V., Abril, G., Darchambeau, F., Teodoru, C. R., Deborde, J., Vidal, L. O., Lambert, T. and Bouillon, S. (2015). Divergent biophysical controls of aquatic CO2 and CH4 in the World's two largest rivers. Scientific reports, 5.

Carlson, C.A. (2002). Production and removal processes. Pp. 91–151 in Biogeochemistry of Marine Dissolved Organic Matter. D.A. Hansell and C.A. Carlson, eds, Academic Press, San Diego, CA.

Ciais, P., Sabine C., Bala, G., Bopp, L., Brovkin, V., Canadell, J., Chhabra, A., DeFries, R., Galloway, J., Heimann, M., Jones C., , Le Quéré, C., Myneni, R.B., Piao, S., and Thornton, P., (2013). Carbon and Other Biogeochemical Cycles. In: Climate Change 2013: The Physical Science Basis. Contribution of Working Group I to the Fifth Assessment Report of the Intergovernmental Panel on Climate Change [Stock-

er, T.F., D. Qin, G.-K. Plattner, M. Tignor, S.K. Allen, J. Boschung, A. Nauels, Y. Xia, V. Bex and P.M. Midgley (eds.)]. Cambridge University Press, Cambridge, United Kingdom and New York, NY, USA.

Cole, J. J., Prairie, Y. T., Caraco, N. F., McDowell, W. H., Tranvik, L. J., Striegl, R. G., Duarte, C.M., Kortelainen, P., Downing, J.A., Middelburg, J.J. and Melack, J. (2007). Plumbing the global carbon cycle: integrating inland waters into the terrestrial carbon budget. Ecosystems, 10(1), 172-185.

Cole, J. J. and Prairie, Y. T. (2009). Dissolved CO2. In: Gene E. Likens, (Editor) Encyclopedia of Inland Waters. volume 2, pp. 30-34 Oxford: Elsevier.

Dickson, A.G. and Goyet, C. (1994). Handbook of methods for the analysis of the various parameters of the carbon dioxide system in sea water, DOE, version 2, ORNL/CDIAC-74.

Dickson, A. G., Sabine, C. L., & Christian, J. R. (2007). Guide to Best Practices for Ocean CO2 Measurements.

Encyclopædia Britannica, The Editors of Encyclopædia Britannica (1998). Rajang River. URL: https://www.britannica.com/place/Rajang-River (Last visited on March 2017)

Gastaldo, R. A. (2010). Peat or no peat: Why do the Rajang and Mahakam Deltas differ?. International Journal of Coal Geology, 83(2), 162-172.

Del Giorgio, P. A. and Davis, J. (2003). Patterns in dissolved organic matter lability and consumption across aquatic ecosystems. Aquatic ecosystems: interactivity of dissolved organic matter, 399-424.

Del Giorgio, P. A. and Williams, P. J. L. B. (Eds.). (2005). Respiration in aquatic ecosystems. Oxford University Press, USA.

Harun, S., Dambul, R., Abdullah, M. H. and Mohamed, M. (2014). Spatial and seasonal variations in surface water quality of the Lower Kinabatangan River Catchment, Sabah, Malaysia. Journal of Tropical Biology & Conservation (JTBC), 11.

Hope, D., Billett, M. F., & Cresser, M. S. (1994). A review of the export of carbon in river water: fluxes and processes. Environmental pollution, 84(3), 301-324.

Hopkinson, C., Vallino, J., Nolin, A. (2002). Decomposition of dissolved organic matter from the continental margin. Deep Sea Research Part II: Topical Studies in Oceanography. 49. 4461-4478.

Johnson, J. E. (1999). Evaluation of a seawater equilibrator for shipboard analysis of dissolved oceanic trace gases. Analytica chimica acta, 395(1), 119-132.

Koehler, B., Wachenfeldt, E., Kothawala, D., & Tranvik, L. J. (2012). Reactivity continuum of dissolved organic carbon decomposition in lake water. Journal of Geophysical Research: Biogeosciences, 117(G1).

Lauerwald, R., Laruelle, G. G., Hartmann, J., Ciais, P., & Regnier, P. A. (2015). Spatial patterns in CO2 evasion from the global river network. Global Biogeochemical Cycles, 29(5), 534-554.

Le, T. P. Q., Dao, V. N., Rochelle-Newall, E., Garnier, J., Lu, X., Billen, G., Duong, T. T., Ho, C. T., Etcheber, H., Nguyen, T. M. H., Nguyen, T. B. N., Nguyen, B. T., Da Le, N., and Pham, Q. L. (2017) Total organic carbon fluxes of the Red River system (Vietnam). Earth Surf. Process. Landforms, 42: 1329–1341.

LICOR. (2002). Li-820 CO2 Analyser Instuction Manual. LI-COR, Inc., 4421 Superior Street, Lincoln.

Likens, G. E. (2010). River Ecosystem Ecology: A Global Perspective. Academic Press.

Malaysian Meteorological Department. URL: http://www.met.gov.my/en/web/metmalaysia/climate/generalinformation/malaysia (Last visited on March, 2017).

McCauley, A., Jones, C., Oslon-Rutz, K. (2017). Soil pH and organic matter. Nutrient Management. Module No.8

Moore, S., Gauci, V., Evans, C. D., and Page, S. E. (2011). Fluvial organic carbon losses from a Bornean blackwater river. Biogeosciences, 8(4), 901-909.

Moran, M. A., Sheldon, W. M., & Sheldon, J. E. (1999). Biodegradation of riverine dissolved organic carbon in five estuaries of the southeastern United States. Estuaries and Coasts, 22(1), 55-64.

Müller, D., Warneke, T., Rixen, T., Müller, M., Jamahari, S., Denis, N., Mujahid, A. and Notholt, J. (2015). Lateral carbon fluxes and CO_2 outgassing from a tropical peat-draining river. Biogeosciences, 12(20), 5967-5979.

Müller-Dum, D., Warneke, T., Rixen, T., Müller, M., Christodoulou, A., Baum, A., and Notholt, J. Carbon fluxes from the Rajang River, Malaysia, influenced by peat and human activity. Submitted to Journal of Hydrology: Regional Studies (on March 9th, 2017).

National Oceanic & Atmospheric Administration (NOAA), Earth System Research Laboratory (2017), URL: https://www.esrl.noaa.gov/gmd/ccgg/trends/ (last visited on March, 2017)

Pollard, P. C. (2013). In situ rapid measures of total respiration rate capture the super labile DOC bacterial substrates of freshwater. Limnology and Oceanography: Methods, 11(11), 584-593.

Pörtner, H. O. (2008). Ecosystem effects of ocean acidification in times of ocean warming: a physiologist's view. Marine Ecology Progress Series, 373, 203-218.

Prairie, Y. T., and Cole, J. J. (2009). Carbon, unifying currency. Encyclopedia of Inland Waters. 1st ed. Oxford: Academic Press2009, 743-6.

Richey, J. E., Melack, J. M., Aufdenkampe, A. K., Ballester, V. M., and Hess, L. L. (2002). Outgassing from Amazonian rivers and wetlands as a large tropical source of atmospheric CO2. Nature, 416(6881), 617-620.

Raymond, P. A., Hartmann, J., Lauerwald, R., Sobek, S., McDonald, C., Hoover, M., Butman, D., Striegl, R., Mayorga, E., Humborg, C., Kortelainen, P., Dürr, H., Meybeck, M., Ciais, P. and Guth P. (2013). Global carbon dioxide emissions from inland waters. Nature, 503(7476), 355-359.

Regnier, P., Friedlingstein, P., Ciais, P., Mackenzie, F. T., Gruber, N., Janssens, I. A., Laruelle, G., Lauerwald, R., Luyssaert, S., Andersson, A., Arndt, S., Arnosti, C., Borges, A., Dale, A., Gallego-Sala, A., Goddéris, Y., Goossens, N., Hartmann, J., Heinze, C., Ilyina, T., Joos, F., LaRowe, D., Leifeld, J., Meysman, F., Munhoven, G., Raymond, P., Spahni, R., Suntharalingam, P. and Thullner, M. (2013). Anthropogenic perturbation of the carbon fluxes from land to ocean. Nature geoscience, 6(8), 597-607.

Riebeek H. (2011). Design by Robert Simmon June 16, 2011 Nasa

Rixen, T., Baum, A., Wit, F. and Samiaji, J. (2016). Carbon Leaching from Tropical Peat Soils and Consequences for Carbon Balances. Frontiers in Earth Science, 4, 74.

Robins, P. E., Skov, M. W., Lewis, M. J., Giménez, L., Davies, A. G., Malham, S. K., Neill, S.P., McDonald, J.E., Whitton, T.A., Jackson, S.E. and Jago, C. F. (2016). Impact of climate change on UK estuaries: A review of past trends and potential projections. Estuarine, Coastal and Shelf Science, 169, 119-135.

Schulz, K. G., Riebesell, U., Rost, B., Thoms, S., & Zeebe, R. E. (2006). Determination of the rate constants for the carbon dioxide to bicarbonate inter-conversion in pH-buffered seawater systems. Marine chemistry, 100(1), 53-65.

Schulze-Makuch, D. and Irwin, L.N. (2004 hard cover, 2006 soft cover). Life in the Universe: Expectations and Constraints. Springer, Berlin, 172 p. (Academic Science Book)

Strack, M. (Ed.) (2008). Peatlands and climate change. IPS, International Peat Society.

Staub, J. R., Among, H. L. And Gastaldo, R. A. (2000). Seasonal sediment transport and deposition in the Rajang River delta, Sarawak, East Malaysia. Sedimentary Geology, 133(3), 249-264.

Staub, J. R. and Gastaldo, R. A. (2003). Late Quaternary sedimentation and peat development in the Rajang River delta, Sarawak, east Malaysia.

Thurman, E. M. (1985). Aquatic humic substances. In Organic geochemistry of natural waters (pp. 273-361). Springer Netherlands.

Verdugo, P., Alldredge, A. L., Azam, F., Kirchman, D. L., Passow, U., & Santschi, P. H. (2004). The oceanic gel phase: a bridge in the DOM–POM continuum. Marine Chemistry, 92(1), 67-85.

Wetzel, R. G., & Likens, G. E. (1991). Lymnological analyses. New York, Springer-Verlag.

Wiesler, F., and Sodaro, R. (1996). Degasification of water using novel membrane technology. Ultrapure Water, 13(6), 53-56.

Wit, F., Müller, D., Baum, A., Warneke, T., Pranowo, W. S., Müller, M. and Rixen, T. (2015). The impact of disturbed peatlands on river outgassing in Southeast Asia. Nature communications, 6, 10155.

Zeebe, R. E., and Wolf-Gladrow, D. A. (2001). CO2 in seawater: equilibrium, kinetics, isotopes (No. 65). Gulf Professional Publishing.